

1 **Reprocessing of XBT profiles from the Ligurian and Tyrrhenian seas over the**
2 **time period 1999-2019 with full metadata upgrade**

3 Simona Simoncelli¹, Franco Reseghetti^{2,§}, Claudia Fratianni¹, Lijing Cheng^{3,4}, Giancarlo Raiteri²

4 ¹ Istituto Nazionale di Geofisica e Vulcanologia (INGV), Viale Berti Pichat 6/2, 40127 Bologna, Italy,

5 <https://ror.org/029w2re51>;

6 ² [Italian National Agency for New Technologies, Energy and Sustainable Economic Development \(ENEA\)](#), S.

7 Teresa Marine Research Centre, 19032 Pozzuolo di Lerici, Italy;

8 ³ International Center for Climate and Environment Sciences, Institute of Atmospheric Physics, Chinese

9 Academy of Sciences, Beijing, 100029, China;

10 ⁴ Center for Ocean Mega-Science, Chinese Academy of Sciences, Qingdao, 266071, China;

11 [§] [Now at Istituto Nazionale di Geofisica e Vulcanologia \(INGV\), Viale Berti Pichat 6/2, 40127 Bologna, Italy](#);

12 *Correspondence to:* Simona Simoncelli (simona.simoncelli@ingv.it)

13 **Abstract**

14 The advent of open science and the United Nations Decade of Ocean Science for Sustainable Development
15 are revolutionizing the ocean data sharing landscape for an efficient and transparent ocean information and
16 knowledge generation. This blue revolution raised awareness on the importance of metadata and community
17 standards to activate interoperability of the digital assets (data and services) and guarantee that data driven
18 science preserve provenance, lineage and quality information for its replicability. Historical data are frequently
19 not compliant with these criteria, lacking metadata information that was not retained crucial at the time of the
20 data generation and further ingestion into marine data infrastructures. The present data review is an example
21 attempt to fill this gap through a thorough data reprocessing starting from the original raw data and operational
22 log sheets. The data gathered using XBT (eXpendable BathyThermograph) probes during several monitoring
23 activities in the Tyrrhenian and Ligurian Seas between 1999 and 2019 have been first formatted and
24 standardized according to the latest community best practices and all available metadata have been inserted,
25 including calibration information never applied, uncertainty specification and bias correction from Cheng et
26 al. (2014). Secondly, a new automatic Quality Control (QC) procedure has been developed and a new
27 interpolation scheme applied. The reprocessed (REP) dataset has been compared to the data version, presently
28 available from SeaDataNet (SDN) data access portal, processed according to the pioneering work of Manzella
29 et al. (2003) conducted in the framework of the EU Mediterranean Forecasting System Pilot Project (Pinardi
30 et al., 2003). The comparison between REP and SDN datasets has the objective to highlight the main
31 differences derived from the new data processing. The maximum discrepancy among the REP and SDN data
32 versions resides always within the surface layer (REP profiles are warmer than SDN ones) until 150 m depth,
33 generally when the thermocline settles (from June to November). The overall bias and root mean square
34 difference are equal to 0.002 °C and 0.041 °C, respectively. Such differences are mainly due to the new
35 interpolation technique (Barker and McDougall, 2020), and the application of the calibration correction in the
36 REP dataset.

Deleted: actionate

Deleted: present

Deleted: through the saved query Url
https://cdi.seadatanet.org/search/welcome.php?query=1866&query_code={4E510DE6-CB22-47D5-B221-7275100CAB7F}

Deleted: May

Deleted: , the lack of filtering

45 The REP dataset (Reseghetti et al., 2024; https://doi.org/10.13127/rep_xbt_1999_2019.2) is available and
46 accessible through the INGV ([Istituto Nazionale di Geofisica e Vulcanologia, Bologna](http://www.ingv.it)) ERDDAP
47 ([Environmental Research Division's Data Access Program](http://ocean.bo.ingv.it/erddap/index.html)) server, which allows machine to machine data
48 access in compliance with the FAIR (Findable, Accessible, Interoperable and Reusable) principles (Wilkinson
49 et al., 2016).

Deleted: 3

Deleted: https://doi.org/10.13127/rep_xbt_1999_2019

Deleted: (<http://ocean.bo.ingv.it/erddap/index.html>)

Deleted: Interoperable,

50 1 Introduction

51 The open science paradigm boosted the sharing of data through different pathways determining the generation
52 of different versions of the same datasets. This might depend on the timeliness of data delivery, either in Near
53 Real Time (NRT) or Delayed Mode (DM), the data center managing the dataset, the data assembly center or
54 the marine data infrastructure collating it. The awareness of the importance of a complete metadata description
55 is increasing among the scientific community since it allows interoperability, traceability of the data lifecycle,
56 transparency and replicability of the knowledge generation process. In particular, some key information is
57 crucial in climate science because it allows reanalysis of historical data, quantifying and reducing uncertainties,
58 which are used to derive accurate scientific knowledge (Simoncelli et al., 2022).

Deleted: to re-analyze

59 The data provider should define the overall quality assurance strategy along with the data lifecycle to guarantee
60 the availability of the best data product, which implies the possibility of reprocessing the dataset according to
61 the state-of-the-art Quality Control (QC) procedures and standards. Data driven research should use the most
62 extensive datasets with complete metadata information passed through a trustworthy QC procedure. These are
63 also basic requirements to guarantee data reusability once the data are made openly accessible. The complete
64 set of metadata assures transparency of the data provenance and avoids the circulation of multiple versions.

65 The integration in global databases of data not compliant with these principles emerged recently for
66 measurements gathered in the last century, when the importance of storing data with complete ancillary
67 information was not yet clear. A striking example is provided by the XBT (eXpendable BathyThermograph)
68 probes, the oceanographic instruments that recorded the largest number of temperature profiles in the ocean
69 from the 1970s to the 1990s (Meyssignac et al., 2019). The complete metadata information is crucial for QC,
70 data reprocessing (Cheng et al., 2014; 2018; Goni et al., 2019) and integration with other data types to estimate
71 key ocean monitoring indicators, such as the trend of global ocean heat content (Cheng et al., 2020; 2021;
72 2022), one of the most important climate change indicators. According to the literature (Cheng et al., 2016 and
73 2017; Parks et al., 2022), the crucial metadata information that must be associated with XBT data includes
74 probe type and manufacturer, fall rate equation, launch height, and recording system. This information was
75 not mandatory for the data ingestion in the main marine data infrastructure, thus most historical data miss it.
76 For example, 50% of XBT profiles in the World Ocean Database (WOD) have no information about
77 manufacturer or probe type (Cawley et al. 2021), necessitating the application of intelligent metadata
78 techniques to complement it (Palmer et al., 2018; Leahy et al., 2018; Haddad et al., 2022).

Deleted: quality control

79 This data review originated from the recognition that the historical XBTs from the Ligurian and Tyrrhenian
80 Seas, presently available in the main marine data infrastructures - SDN (<https://www.seadatanet.org/>), WOD

Deleted: This data review originated from the recognition that the present version of historical XBTs from the Ligurian and Tyrrhenian Seas, available through some main marine data infrastructures, SeaDataNet (<https://www.seadatanet.org/>), World Ocean Database (<https://www.ncei.noaa.gov/products/world-ocean-database>), Copernicus Marine Service (CMS, <https://marine.copernicus.eu/>), might differ and have incomplete metadata description.

96 (<https://www.ncei.noaa.gov/products/world-ocean-database>), [Copernicus Marine Service \(CMS,](https://marine.copernicus.eu/)
97 <https://marine.copernicus.eu/>) - have incomplete metadata description and the data might also differ. Our
98 objective was to recover the raw data together with the full metadata description and secure them to the future
99 generation of scientists for their further use. This awareness raised contemporary to the evolution of open
100 science and FAIR (Findable, Accessible, Interoperable and Reusable) data management principles, which
101 motivated us to adopt the latest community standards, QC procedures, and to implement an ERDDAP server
102 as data dissemination strategy. ERDDAP is an open source environmental data server software developed by
103 NOAA and used throughout the ocean observing community (Pinardi et al. 2019; Tanhua et al. 2019) which
104 allows us to become a node of the present data digital ecosystem, in line with one of the expected societal
105 outcomes (“transparent and accessible” ocean) of the UN Decade of Ocean Science 2021-2030 (Ryabinin et
106 al., 2019; Simoncelli et al., 2022).
107 The paper describes the reprocessing of temperature profiles from expendable probes deployed between 1999
108 and 2019 in the Ligurian and Tyrrhenian seas, most of them from vessels operating a commercial line between
109 the Italian ports of Genova and Palermo within the Ships Of Opportunity Program (SOOP) of the Global Ocean
110 Observing System (GOOS), currently identified as MX04 line. Additional XBT data were collected through
111 ancillary monitoring surveys with commercial and research vessels. The dataset contains some XCTD
112 (eXpendable Conductivity-Temperature-Depth probes) profiles (less than 1%) too. The reprocessed dataset
113 (REP) is obtained from the original raw XBT profiles, the readable output of the Data Acquisition System
114 (DAQ). A correction based on the DAQ calibration (when available) is applied to each temperature recorded
115 value but also provided as separate information, to allow the user to eventually subtract it. Automated QC
116 tests, specifically tuned for western Mediterranean basins, based on the latest documented QC procedures
117 (Cowley et al., 2022; Parks et al., 2022; Good et al., 2023; Tan et al., 2023) and best practices to assign a
118 Quality Flag (QF) are applied, followed by interpolation of raw profiles at each meter depth. All available
119 information collected during data-taking has been added in the metadata section, according to the SeaDataNet
120 standards (<https://www.seadatanet.org/Standards>) and IQuOD (International Quality-controlled Ocean
121 Database, <https://www.iquod.org/index.html>) recommendations. Uncertainty specification for both depth and
122 temperature is also provided, being a crucial information for assimilating data in ocean reanalysis or for
123 utilizing them in downstream applications. Cheng et al. (2014) demonstrated that XBT data are characterized
124 by systematic bias when compared with data gathered from CTD, and computed the commonly used correction
125 scheme for both temperature and depth records, which is very important to derive integrated data products or
126 ocean indicators from multiple data sources and instruments (Cheng et al., 2016). The REP dataset includes
127 Cheng et al. (2014) correction scheme applied to the calibrated profiles at original depth and then interpolated
128 at each meter depth.
129 The REP data product allows the user to select from the original profiles to the validated, interpolated and
130 corrected ones, filtering on the basis of the required quality level, selecting the associated QF. Furthermore,
131 the dataset is accessible through the ERDDAP (Environmental Research Division's Data Access Program) data

Deleted: Quality Control (

Deleted:)

Deleted:

Deleted: recorded

Deleted: ro-pax (Roll-on/roll-off Passengers)

Deleted: (

Deleted:

Deleted: s

Deleted: a 1 m in

Deleted: (SDN)

Deleted: and

Deleted: Quality Flags (QF)

Deleted: with both the raw and the interpolated data

145 server (<http://oceano.bo.ingv.it/erddap/index.html>) installed at INGV (<https://ror.org/029w2re51>) which
146 provides a simple and consistent way to download it in several common file formats.

147 This study was conducted in the framework of the MACMAP (Multidisciplinary Analysis of Climate change
148 indicators in the Mediterranean And Polar regions) project ([https://progetti.ingv.it/it/progetti-](https://progetti.ingv.it/it/progetti-dipartimentali/ambiente/macmap)
149 [dipartimentali/ambiente/macmap](https://progetti.ingv.it/it/progetti-dipartimentali/ambiente/macmap)) funded by INGV (<https://ror.org/00qps9a02>) (2020-2024) in technical
150 collaboration with ENEA ([Italian National Agency for New Technologies, Energy and Sustainable Economic](#)
151 [Development](#)) and GNV (Grandi Navi Veloci) shipping company. In fact, the reprocessing of the historical
152 XBTs was preparatory to the automatic validation, management and publication of new XBT data gathered on
153 the MX04 line from September 2021, after two years interruption of the monitoring activity.

154 The paper is organized as follows: Section 2 describes the main characteristics of an XBT system; Section 3
155 describes the original dataset and the monitoring activities that sustained it; Section 4 describes the
156 methodology applied for the automatic QC and the correction derived from calibration; Section 5 is about the
157 results; Section 6 summarizes the main results and draws conclusions; Section 7 describes the REP dataset
158 findability and accessibility.

159 2 The XBT system

160 In the early 1960s, following a request from the US Navy looking for a seawater temperature profiler for
161 military applications, engineers from Francis Associates developed an early version of an XBT probe. The
162 prototype was improved within Sippican Corp. (now part of Lockheed Martin Co., hereinafter Sippican) and
163 then adopted by the US Navy (Reid, 1964; Arthur D. Little, 1965 and 1966). Within a few years Sippican
164 optimized the original project and marketed different XBT types with specifications suitable for various depths
165 and ship speed. XBTs became very popular within the oceanographic community (Flierl and Robinson, 1977)
166 allowing the gathering of Temperature (T) profiles through the use of commercial vessels (ships of
167 opportunity) and not just research vessels.

168 The XBT system consists of: an expendable ballistic probe falling into seawater; a device (DAQ) that records
169 an electrical signal and converts it into usable numerical data (in combination with a computer unit) and the
170 connection between the falling probe and the DAQ (e.g. Goni et al., 2019 and Parks et al., 2022). The sensing
171 component is an NTC (Negative Temperature Coefficient) thermistor that changes its resistance according to
172 the temperature of seawater flowing through the central hole of the probe nose where it is located. Its thermal
173 time constant τ (time needed to detect 63% of a thermal step signal) is ~ 0.11 s (Magruder, 1970 and references
174 therein) so a time of ~ 0.6 s is needed to detect a step temperature change. Technical characteristics required
175 by Sippican for the NTC thermistor, reading circuit and resistance to temperature conversion procedure (e.g.
176 Sippican 1991 and Appendix A), put some limits on the accuracy of XBT measurements.

177 Another essential component is the thin twin copper wire which is part of the acquisition circuit and which is
178 unwound by two spools simultaneously (clockwise from the ship and counterclockwise from the falling probe),
179 a technique which decouples the XBT vertical motion from the translational motion of the ship. The albeit
180 weak electric current that runs through the wire during acquisition transforms the wire into a large antenna

Deleted:

Deleted: (GNV)

Deleted:

Deleted: , its accuracy, resolution and uncertainties

Deleted: American

Deleted: , who thereafter founded the Sippican Co. (now part of the Lockheed Martin Co., hereinafter Sippican), developed the first version of today's XBT probes following to a US Navy call for a seawater temperature (T) profiler for military applications

Deleted: probe

Deleted: variable

Deleted:

Deleted: (mounted inside the ballistic probe),

Deleted: T

Deleted: zinc

Deleted:

Deleted: in the range 0.080 - 0.130 s (so that five-tau rule indicates a time of about 0.5 s to almost fully detect a step temperature change)

Deleted: used

Deleted: (whose features and performances remained unchanged since the early 1960s)

Deleted: high

Deleted: with XBT probes

Deleted: double

Deleted: in

Deleted: in

Deleted: falling

Deleted: through the seawater

211 sensitive to nearby electromagnetic phenomena. A non-uniform coating application and a defective winding
 212 on one of the spools cause a significant part of the faulty or prematurely terminated acquisitions.
 213 XBT probes do not house any pressure sensor and the depth associated with a temperature measurement is not
 214 measured directly but estimated by a Fall Rate Equation (FRE) provided by the manufacturer with coefficients
 215 that depend on the probe type and are valid for the world ocean. The software transforms a time series of
 216 resistance values sensed by the thermistor into a series of depth - T values using first a resistance-to-
 217 temperature conversion relationship (identical for all XBT types because it is specific for the thermistor used,
 218 see Appendix A) and then calculating the corresponding depth values by applying a specific FRE for each
 219 probe type. Sippican has preset conservative values for the recording time in its acquisition software but these
 220 values can be freely modified in order to use all the wire wound on the probe spools. The first column of Table
 221 1 shows the nominal values and the maximum recorded depth in the same areas for each specific probe type.
 222
 223 Each component of an XBT system contributes to the overall uncertainty on depth and T measurements.
 224 Recently the IQuOD group (Cowley et al., 2021) released a summary of T uncertainties specifications for
 225 different oceanographic devices determined using available knowledge (Type B uncertainty). The uncertainty
 226 estimate associated with XBT probes adopts the accuracy values provided by the manufacturer:

- 227 • for depth: 4.6 m up to 230 m depth and 2% at greater depths;
- 228 • for T: within the range 0.1 - 0.2 °C, with small variations depending on the manufacturer and the
 229 manufacturing date. The value associated with the XBT probes in the REP dataset is equal to 0.10 °C.

230 Bordone et al. (2020) compared XBT profiles from SOOP activities in the Ligurian and Tyrrhenian Sea with
 231 quasi contemporaneous (± 1 day) and co-located (distance smaller than 12 km) Argo profiles. The XBT
 232 profiles used by Bordone et al. (2020) are included in the REP dataset but they went through a different QC
 233 and interpolation procedure that could slightly modify their results. In the 0-100 m layer, the mean T difference
 234 was 0.24 °C (the median 0.09 °C) and the Standard Deviation (SD) was 0.67 °C. Below 100 m depth, the XBT
 235 measurements were on average 0.05 °C warmer than the corresponding Argo values (mean and median were
 236 almost coincident) and the SD was 0.10°C. This last SD value agrees with the manufacturer specification and
 237 the T uncertainty value reported by Cowley et al. (2021), which has been assigned to the REP data. The values
 238 estimated by Bordone et al. (2020) for the surface and sub-surface layer (depth < 100 m) are instead affected
 239 by both the XBT (4.6 m) and Argo (2.4 dbar) depth uncertainty estimation, meaning that a small variation in
 240 depth could correspond to a large variation in temperature especially when the seasonal thermocline develops,
 241 so that the comparison with Argo values would not be significant. The specified uncertainties are independent
 242 of the systematic error or bias affecting the XBT temperature and depth measurements, that have been
 243 corrected in the REP dataset applying the Cheng et al. (2014) correction scheme.
 244
 245 In fact, the first part of the XBT motion is critical, meaning that the T and depth values in the surface layer
 246 must be considered very carefully, especially if the launch height (which influences the entry velocity of the
 247 probe and consequently the time and depth at which it reaches the terminal velocity, i.e. the value used in the

Deleted: The
 Deleted: of the insulating substance on the wire
 Deleted: its
 Deleted: are the
 Deleted: of
 Deleted: interrupted
 Deleted:
 Deleted: phenomenological
 Deleted: which

Deleted: The software transforms a time series of resistance values provided by the DAQ into a series of depth - T values using first a resistance-to-temperature conversion relationship (identical for all XBT types because it is specific for the thermistor used, see Appendix A) and thus applying the coefficients of a FRE specific to each probe

Deleted: measurement accuracy
 Deleted: values

Deleted: According to Anderson (1980): "Sippican specifies the system with a stated worst case temperature accuracy ± 0.2 °C (± 0.1 °C for the probe and ± 0.1 °C for a properly maintained and calibrated recorder... and depth accuracy at ± 15 feet (4.6 m) or $\pm 2\%$, whichever is larger". Recently the IQuOD group (Cowley et al., 2021) released a summary of uncertainties on T and depth values of different oceanographic devices, and the reported value for XBTs is in the range 0.1-0.2 °C and slightly depending on the manufacturer and the manufacturing date.

Deleted: ¶

Deleted: In Bordone et al. (2020) it was found that the XBT measurements in the Mediterranean below 100 m compared to those of almost contemporaneous and co-located Argo profilers (in order to have a practically unchanged measurand) are warmer by about 0.05 °C and with a value of 0.10°C as the standard uncertainty of XBT measurements after correction obtained by comparing them with Argo profiles and which was later used in the QC as the SD for the XBT values.¶

Deleted: T
 Deleted: fall

287 FRE) differs from 3 m above sea level, the value suggested by Sippican. Very high launch platforms make the
 288 initial depth values calculated through the FRE incorrect (Bringas and Goni, 2015 and references therein). In
 289 addition, the time constant of the thermistor (Magruder, 1970 and references therein), the thermal mass of the
 290 XBT probe (e.g. Roemmich and Cornuelle, 1987) and the storage temperature, influence the reliability of the
 291 first T records. For these reasons, careful data validation in the near surface layer and where the seasonal
 292 thermocline occurs (i.e. depths shallower than 100 m in the study region), is crucial.

293 The depth resolution depends both on DAQ sampling rate and FRE of the XBT probe. All DAQ models used
 294 in this dataset work at 10 Hz (i.e. a sample every 0.1 s, a time interval nearly coincident with the time constant
 295 of the NTC thermistor) so that the depth resolution has actual values close to 0.6 m. The T_v resolution is usually
 296 0.01 °C when using the standard Sippican software while 0.001 °C is the standard output for Devil/Quoll
 297 DAQs and some old Sippican software versions. Throughout the work, three decimal digits are always used
 298 for T values and the derived quantities (i.e. vertical gradient). The computer clock (always updated to the UTC
 299 value shortly before the start/after the end of operations) provides the time coordinate of each profile with a
 300 sensitivity of 1 s. The differences recorded with respect to the standard UTC time have always been smaller
 301 than 1 s over a 24 hour time frame.

302 Sippican's manuals released over the years (e.g. Sippican 1968, 1980, 1991, 2006, 2010 and 2014) and reports
 303 (e.g. Sy, 1991; Cook and Sy, 2001; Sy and Wright, 2001; Parks et al., 2022) well describe the best practices
 304 for XBT use. The checking of the XBT system with a tester before and after data collection as well as the
 305 complete description of the system characteristics in the metadata is highly recommended for an optimal use
 306 of XBT measurements. When strip chart recorders were used, a preliminary and accurate calibration of the
 307 acquisition unit with a tester was mandatory (e.g. Sippican, 1968 and 1980; Plessey-Sippican, 1975). With the
 308 advent of digital systems this procedure was also recommended (Bailey et al., 1994). Only since July 2010 the
 309 tester check has been introduced in the monitoring activity along the MX04 line and few other subsets of
 310 profiles contained in the REP dataset. Reseghetti et al. (2018) found a reduction of the (XBT-CTD) temperature
 311 difference after introducing a correction based on the tester check. This was also confirmed by the comparison
 312 between XBT and Argo profiles described in Bordone et al. (2020). Based on these findings, a specific
 313 correction has been developed and it represents a key component of the information never used in previous
 314 data versions and unlocked in the REP dataset (section 4.3).

315 The first XCTD models were developed by Sippican (Sippican, 1983) in the 1980s and were analog. They
 316 were completely replaced in the last years of the last century by digital versions produced by the Japanese
 317 company TSK (Tsurumi Seiki Co.). XCTD-1 probes present some differences compared to XBTs in terms of
 318 resolution and accuracy, and a completely different recording circuitry. The manufacturer (the Japanese
 319 company TSK) claims an accuracy of 0.02 °C on T_v (a factor of five better than XBTs) and a resolution of 0.01
 320 °C while the depth accuracy is the same as for XBT probes. The sampling frequency is 25 Hz (i.e. a reading
 321 of the thermistor resistance value every 0.04 s), with a falling speed which is just over half that of the XBT probes
 322 (see Table 1), the depth resolution for the model XCTD-1 is about 0.14 m.

Deleted: and hard to describe: a probe needs a few seconds from when it hits the sea surface to make its motion stable (a few tens of meters, given its falling speed of about 6 ms⁻¹, Bringas and Goni, 2015).

Deleted: i

Deleted:

Deleted: analyzed basin of the Mediterranean Sea

Deleted: Below the thermocline, or in the surface layer in the cold periods (due to homogeneous temperature values), the nominal poor depth accuracy for XBT data does not affect the whole quality too much. †

Deleted: depends on specific FRE with

Deleted: reading

Deleted: (both raw and interpolated)

Deleted: close to

Deleted: , which corresponds to the instrument sensitivity, in a time interval of one day

Deleted:

Deleted: canist

Deleted: binding

Deleted: subsequent

Deleted: the

Deleted: The evaluation of the performances of the XBT system during data collection is a needed step to improve the quality.

Deleted: canist

Deleted: (an integral component of an XBT system, tester hereafter)

Deleted: but this good practice has been frequently disregarded over the years

Deleted: This operational procedure has been applied

Deleted: o

Deleted: to

Deleted: to

Deleted: improvements described by Reseghetti et al. (2018),

Deleted: is

Deleted: As for the

Deleted: , there are

Deleted: the

Deleted: temperature

Deleted: estimated uncertainty on the

Deleted: for the

Deleted: (i.e. 4.6 m or 2%, whichever is greater)

Deleted: ,

Deleted: and, thanks to

Deleted: of

Deleted: of

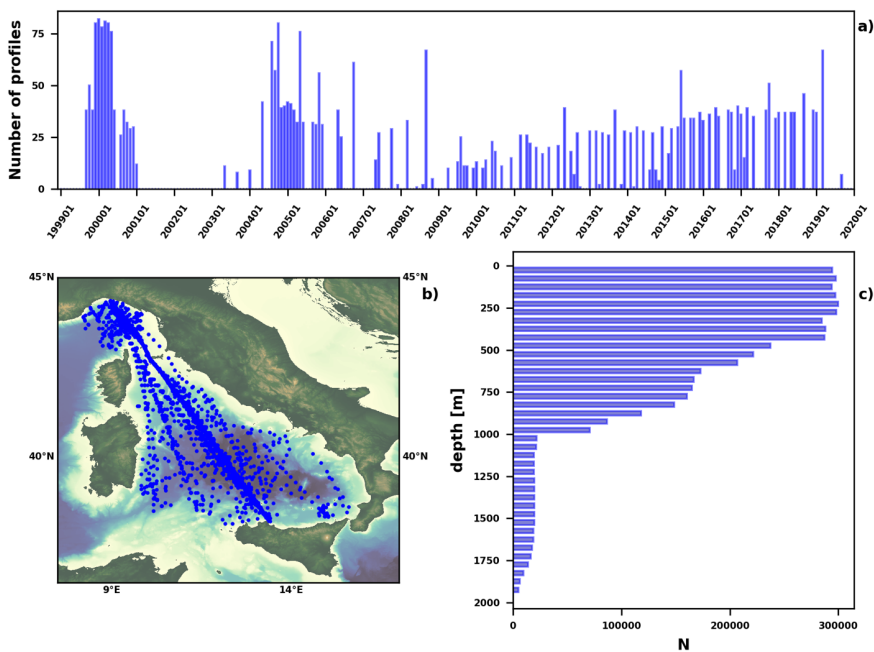
371 **3 The dataset**

372 3782 temperature profiles collected from September 1999 to September 2019 in operations managed by
373 ENEA (S. Teresa Marine Research Centre, STE thereafter) mainly through the use of commercial ships, are
374 included in the REP dataset. They come from XBT probes, plus a few dozen XCTDs. Figure 1 shows the XBT
375 profiles temporal and spatial distribution, highlighting their sparseness, mainly influenced by the irregular
376 monitoring activity and data concentration along the MX04 Genova-Palermo line. The vertical data
377 distribution (Figure 1c) is also non-homogeneous due to the local bathymetry, the use of different probe types
378 and the ship speed.

Deleted: 57

Deleted: of

Deleted: , which may affect the duration of the data acquisition



380
381 **Figure 1 (a) temporal distribution of the REP (reprocessed) XBT profiles; (b) geographical location; (c) vertical**
382 **distribution in layers of 50 m of depth.**

383 Table 1 shows some of the characteristics of the expendable probes used in this dataset, the FRE coefficients
384 applied to calculate the depth and the mass of the various components of each probe type (ZAMAK - Zink
385 Aluminium Magnesium Kupfer - for the nose, plastic for the body and spool and copper wire, considering the
386 total quantity that can unwind from the on-board spool), which allows to evaluate the overall quantity of
387 material abandoned at sea caused by the REP dataset. We have no information regarding the components of
388 the XCTD-1 probes but their nose is made of plastic material. Sippican is the manufacturer of all the XBT

Deleted:

Deleted: in plastic

Deleted: including

Deleted: in order

Deleted: launch of these probes

Deleted: various

Deleted: used

400 probes ~~used, while~~ the XCTD-1 probes are manufactured by TSK - Tsurumi Seiki Co. and marketed in Italy
 401 by Sippican.

Deleted: as well as
 Formatted: Not Highlight

402 The profiles were gathered during the following monitoring activities:

- 403 1. SOOP monitoring on the Genova-Palermo MX04 line, which provides the greatest contribution both
- 404 in terms of campaigns (1999-2000, 2004-2006, 2010-2019) and quantity of profiles;
- 405 2. SOOP monitoring in collaboration with CSIRO (~~Commonwealth Scientific and Industrial Research~~
- 406 ~~Organization~~), from 2007 to 2011;
- 407 3. Sporadic additional SOOP monitoring by ENEA-STE in the Mediterranean (2012-2014);
- 408 4. An agreement between ENEA and IIM (Italian Hydrographic Institute of the Navy), (2006 - 2019);
- 409 5. An operational collaboration between ENEA-STE and ~~National Research Council of Italy - Institute~~
- 410 ~~of Marine Sciences~~ (CNR-ISMAR, Lerici), (2000 - 2017).

Deleted: an Australian Government Agency

Deleted: (

411 The main characteristics of the vessels and the instrumentation used for the data collection are summarized in
 412 Appendix B.

413 **Table 1 Characteristics of the different probes used: nominal depth suggested (and guaranteed) by Sippican and**
 414 **experienced maximum depth in the Mediterranean; maximum ship speed suggested by Sippican for an optimal**
 415 **drop; coefficients of Fall Rate Equation $D(t) = At - Bt^2$ used for depth calculation (provided by the manufacturer**
 416 **or by IGOSS, Hanawa et al., 1995); ~~per probe~~ amount of ZAMAK, copper and plastic ~~and the number of probes~~**
 417 **included in the dataset ~~for each probe type~~.**

Formatted: Superscript
 Deleted:
 Deleted: for each probe type;
 Deleted: originally considered and those actually
 Deleted: Maximum
 Formatted Table

Probe type	Rated depth (max depth) (m)	Rated ship speed (knots)	Coeff. A (ms ⁻¹)	Coeff. B (ms ⁻²)	ZAMAK (kg) ± 0.001	Plastic (kg) ± 0.001	Copper (kg) ± 0.002	REP dataset
T4	460 (583)	30	6.691	0.00225	0.613	0.052	0.202	143 6
T5	1830 (2272)	6	6.828	0.00182	0.613	0.125	0.357	61
T5/20	1830 (2248)	20	6.828	0.00182	0.613	0.125	0.726	18 9
T6	460 (588)	15	6.691	0.00225	0.613	0.052	0.158	69
T7	760 (977)	15	6.691	0.00225	0.576	0.052	0.240	6 1
DB	760 (962)	20	6.691	0.00225	0.576	0.052	0.294	175 9
T10	200 (292)	10	6.301	0.00216	0.613	0.052	0.098	17 3
XCTD-1	1100 (1100)	12	3.425432	0.00047	None	NA	0.440	35

Deleted: 2

Deleted: 7

Deleted: 0

Deleted: 47

Deleted: 2

418 The first SOOP in the Mediterranean Sea (September 1999 - December 2000) started in the framework of the
 419 European Mediterranean Forecasting System Pilot Project (MFSP, Pinardi et al., 2003; Manzella et al., 2003;
 420 Pinardi and Coppini, 2010) under INGV coordination to support the development of operational oceanography
 421 forecasting activities through the NRT provision of ocean observations. XBT profiles were collected along
 422 transects crossing the Mediterranean Sea designed to monitor the variability of the main circulation features.
 423

436 The raw profiles were subsampled on board by Argos software (15 inflection points) and quickly inserted into
437 the Global Telecommunication System (GTS) while the full resolution profiles were sent to the ENEA-STE
438 assembly center for QC, interpolation and NRT provision to the forecasting center (e.g. Fusco et al., 2003;
439 Manzella et al., 2003; Zodiatis et al., 2005; Millot and Taupier-Letage, 2005a and 2005b). The MX04 line is
440 the only SOOP line still active in the Mediterranean Sea on seasonal basis, thanks to the MACMAP project
441 and the collaboration with GNV, whose ships connect daily (just under 20 hours sailing at about 22 knots)
442 Genova (44.40 °N, 8.91 °E) to Palermo (38.13 °N, 13.36 °E).
443 Starting from September 1999, 20 campaigns were carried out, in collaboration between CNR-ISMAR and
444 ENEA-STE, with initial monthly monitoring frequency, then every 15 days (December 1999 - May 2000), and
445 again monthly frequency until December 2000. T4 probes (with some T6 probes) were launched at fixed
446 intervals of time (every 30 minutes), corresponding to a sampling distance of about 11 nm. A Sippican MK12
447 card inserted into the motherboard of a desktop running Windows 98 IIE and with the software set to stop
448 acquisition at 460 m depth was used. All the campaigns were carried out using the MV "Excelsior", its route
449 was always the same and almost coincident with track 44 of the altimetric satellites (Vignudelli et al., 2003).
450 After a hiatus of more than 3 years and a campaign in May 2004 to check slightly different operational
451 procedures, monitoring along the MX04 line resumed on a monthly basis from September 2004 to December
452 2005 (no cruises in July and August 2005), with two additional cruises in May and October 2006, for a total
453 of 17 campaigns within the EU MFS-Toward Environmental Prediction project (MFS-TEP, Manzella et al.
454 2007; Pinardi and Coppini, 2010). The ships (always GNV vessels) followed a route with marginal differences
455 compared to the previous one due to the introduction of nature conservation limitations in the Tuscan
456 archipelago. In November 2004, February and December 2005 the route was significantly different due to bad
457 weather and sea conditions. The campaigns were planned to travel as close as possible to the passage date of
458 the Jason-1 altimetric satellite along track 44 and for this reason some were carried out on the route traveled
459 in the opposite direction, independently on weather and sea conditions. T4 and DB XBT probes were usually
460 deployed (with a few XCTD-1 and some T6) and the sampling distance was variable from 8 to 12 nm. After a
461 few months, the DAQ (a Sippican MK21 ISA), despite excellent operating conditions and good ground
462 connection, began to record profiles with rapid oscillations (amplitude ≈ 0.05 °C) not attributable to the known
463 water masses characteristics (not shown). Only at the end of the MFS-TEP data taking, careful laboratory
464 checks identified a pair of capacitors on the ISA board as responsible for this malfunction. Unlike MFS-PP,
465 the acquisition software was set to use all the wire available on the probe spool (i.e. 600 m for T4 and 1000 m
466 for DB probes).
467 Monitoring on the MX04 line resumed in July 2010, managed directly by ENEA-STE and until January 2013
468 was widely variable both in terms of frequency and sampling distance (due to the uncertainty in the supply of
469 XBT probes). A regular sampling scheme was then adopted with a launch every 10' of latitude (corresponding
470 to 11-12 nm depending on the ship's course), excluding the archipelago of Toscana, with five to six annual
471 repetitions, following the same route as in 2004-2006 (excluding February 2013 and April 2014 because of
472 very bad weather and sea conditions). It was also decided to carry out monitoring campaigns only with good

Deleted: , using

Deleted: ro-pax (Roll-on/roll-off Passengers) ferries which

Deleted: excluded

Deleted: showed a small degradation and an evident "noise" appeared in the recorded profiles even with

Deleted: path

479 weather and sea conditions. From June 2015, the ships moved to a more westerly route in the northern part of
480 the transect crossing the Corsica Channel (this allows monitoring of the water exchange between the
481 Tyrrhenian Sea and the Ligurian Sea) to rejoin the previous one around at latitude 39°N. The number of drops
482 at fixed positions increased to thirty-seven, mainly DB probes while other XBT types were used in particular
483 areas due to the reduced bathymetry (T10) or with interesting deep thermal structures (T5/20). Based on the
484 experience from XBT vs. CTD comparison tests, since March 2011 the XBT probes were placed in the open
485 air (but always in the shade) for at least half an hour before the deployment to allow them to thermalize with
486 the atmosphere and reduce as much as possible the temperature difference with the sea surface layer.

487 A short SOOP activity in collaboration with CSIRO was completed between December 2007 and March 2011
488 (19 campaigns) using containerships from Hapag Lloyd (namely “Canberra Express”, “Stadt Weimar” and
489 “Wellington Express”) and CMA CGM (“CMA CGM Charcot”) shipping companies, operating between
490 Northern European ports and Australia. These campaigns were characterized by irregular frequency
491 throughout the year, a very high launching platform (25 m over the sea level or more) and a sampling distance
492 between 20 and 35 nm. XBT launches began near the Egadi Islands (west of Sicilia) and terminated in the
493 Corsica Channel, following a path halfway between the MX04 transect and the island of Sardinia. CSIRO
494 installed a Turo Devil DAQ on each vessel while ENEA-STE provided the DB probes.

495 Some additional XBT profiles (mainly DB type) were gathered in the Ligurian Sea between May 2012 and
496 March 2014 on board the GNV ship "Excellent" (in 5 campaigns) and in 2014 two different cruises using a
497 Sippican MK21 USB onboard the container ship “Daniel A” from the Turkish shipping company ARKAS.

498 From 2006 to 2019, 10 campaigns were carried out in collaboration between ENEA and IIM, using the ships
499 "Ammiraglio Magnaghi", "Aretusa" and "Galatea", collecting a total of about 200 profiles using different XBT
500 types, deployed from different heights and using different DAQs.

501 Finally, an operational collaboration between ENEA-STE and CNR-ISMAR allowed to carry out 29
502 campaigns between 2000 and 2017 using vessels managed by the CNR (mainly RV "Urania", but also RV
503 "Minerva Uno" and "Ibis"), gathering several hundred profiles with different XBT probe types deployed from
504 different heights and recorded using four different Sippican DAQ units.

505 The total amount of material abandoned at sea, due to the launch of the XBT/XCTD probes which constitute
506 the REP dataset, is provided using the per-probe values reported in Table 1: over 2300 kg of ZAMAK, 220 kg
507 of plastic material and 1060 kg of copper wire. Furthermore, there was no additional contribution to greenhouse
508 gas emission since mainly commercial vessels were used and, in the case of research vessels, the launch of
509 XBT probes was ancillary to the main activities of the cruise.

510 **4 Methodology**

511 Specific QC procedures for XBT profiles in the Mediterranean Sea were first developed by Manzella et al.
512 (2003) within the MFS-PP project and later improved in Manzella et al. (2007). Temperature observations in
513 the Mediterranean Sea, due to its thermohaline circulation, water mass characteristics and large temperature
514 variability, might present peculiar features like thermal inversions or zero thermal gradient in areas of deep

Deleted: at least

Deleted: eg

Deleted: only

Deleted: es

519 water formation, thus necessitating regional tuning of QC tests. The prior QC procedures included: detection
520 of profile's end, gross range check, position control, elimination of spikes, interpolation at 1 m intervals,
521 Gaussian smoothing, general malfunctioning control, comparison with climatology and final visual check by
522 operator. Some additional constraints were applied: elimination of the initial part of each profile (the first
523 acceptable value is at 4 m depth, following the standard international procedure), allowed temperature values
524 within the 10-30 °C interval, maximum temperature inversion of 4.5 °C in the 0-200 m layer, 1.5 °C below
525 200 m, and 3 °Cm⁻¹ as maximum thermal gradient. This QC has not been applied to the data released in NRT
526 through the GTS (Global Telecommunication System, <https://community.wmo.int/en/activity-areas/global-telecommunication-system-gts>) but only to the data made available in DM through the SDN infrastructure
527 (accessible through the relative saved query from the SDN CDI data access portal at
528 https://cdi.seadatanet.org/search/welcome.php?query=1866&query_code={4E510DE6-CB22-47D5-B221-7275100CAB7F}). The raw data for the GTS dissemination were provided to NOAA and in the early 2000s
529 the profiles were also heavily sub-sampled due to the low bit rate satellite system provided by Argos, the basic
530 GTS data transmission system (Manzella et al., 2003). These different dissemination channels contributed to
531 the existence of several versions of the same profile in different blue data infrastructures (i.e. WOD, SDN).
532 A new automated QC procedure, written in Python and structured as a package, has been implemented in the
533 framework of the MACMAP project starting from the original raw XBT profiles, considering the scientific
534 progress made in the field in the last two decades and the full metadata information available. The aim was
535 twofold: first to secure the best version and most complete dataset for further use to the scientific community;
536 secondly to implement an automated QC workflow for the seasonal XBT campaigns started in September 2021
537 thanks to the MACMAP project. This also allowed to refine and standardize the quality assurance procedures
538 on board of the vessels to record all ancillary information in a pre-defined format and minimize the impact of
539 different operators on the data quality. The calibration correction, detailed in section 4.3, has been added, when
540 available, to the raw data before the QC analysis. However, it is provided as a separate variable associated
541 with each XBT profile and the user can remove it, if required. None of the original data has been deleted but
542 integrated with quality indexes, with the exception of those repeated during data taking, These replicates have
543 been decided by the operator during the sampling activity when the observed profile was affected by serious
544 acquisition problems, both external (i.e. electrical discharge) and probe-specific (wire break or anomalous
545 stretching, insulation penetration, leakage and so on).
546 A final visual check has also been performed using ODV software (R. Schlitzer, Ocean Data View,
547 <https://odv.awi.de/>, 2023) which highlighted the presence of anomalous behavior in some T profiles that the
548 automatic QC tests could not detect. Some examples will be discussed in Section 5 (Figure 10). This visual
549 check suggested assigning to each profile a general QF, choosing between these two options: 1) *excellent*
550 indicating all QC done and 2) *mixed* indicating some problems, with comments to warn the user about the
551 anomalous features.

Deleted: available

Deleted: eventually remove it

Deleted: profiles

Deleted: eliminated

Deleted: and those less than 50 m deep due to problems during acquisition

Formatted: English (US)

Deleted: implemented

Deleted: The REP dataset has been written in ODV format and imported as ODV collection, which contains interpolated temperature profiles and corresponding quality flags of each profile, together with spatio-temporal details, profile name and ship name.

566 **4.1 Automatic Quality Control procedure**

567 The XBT raw profiles have been QCed using a sequence of independent tests, checking for invalid information
 568 on geographic characteristics and for known signatures of spurious measurements. Results of each test are
 569 recorded by inserting the relative **exit value** to the corresponding measurement in **TEMPET01_TEST_QC**
 570 **ancillary variable** according to the scheme shown in Table 2, while Figure 2 provides an example of the QC
 571 tests applied to a profile.

572 The independent QC tests are described hereafter.

573 **Position on land check**

574 The profile position should be located at sea, thus latitude and longitude of each profile is checked against
 575 gridded GEBCO bathymetry (GEBCO Compilation Group, 2022) on a 15 arc-second interval grid to determine
 576 if it is located on land or not: if the “height” is negative it is lower than sea level, and it is flagged as GOOD
 577 (**‘profile is at sea’**), otherwise is flagged as BAD (**‘profile is on land’**).

578 **Depth check**

579 The depth values of each XBT profile are compared to the *last good depth* value provided by the operator.
 580 Depth values are flagged as GOOD (**‘depth is below reference depth value’**) if they are shallower than it
 581 otherwise they are flagged as BAD (**‘depth is above reference depth values’**). The corresponding local bottom
 582 depth extracted from GEBCO and the nominal rated depth by the manufacturer are not used but annotated in
 583 the metadata to facilitate further analysis by expert users.

584 **Table 2 Summary of the automated QC tests and the assigned exit values to each measurement within a profile.**

Test #	Check	Description	Exit value	Exit value description
1	Position control	Function to detect incorrect longitude and latitude values	49/52	49 profile is at sea; 52 profile is on land.
2	Depth	Function to detect depth values out of extreme depths. The reference depth is the depth indicated by the operator.	49/52	49 depth is below reference depth values; 52 depth is above reference depth values
3	Gross range check	Function to detect T values out of ranges in Table 3	49/52	49: T inside the range 52: T is out of range
4	Surface	Function to flag the first 4 meters considering as reference std=0.1 and its growing	49-52	49: T difference < 1 SD 50: 1 SD < T difference < 2 SD 51: 2 SD < T difference < 3 SD 52: T difference > 3 SD
5	vertical gradient	Function to detect stuck values, decreasing and increasing values according to gradient value and considering only the values that passed the previous checks	56-58	56: stuck value 57: negative gradient out of threshold 57#: negative gradient out of threshold in successive iteration (#=1 or 2) 58: positive gradient out of threshold 58#: positive gradient out of threshold in successive iteration (#=1 or 2)
6	wire break/stretch	Function based on vertical gradient check to identify wire break on shipside or on probe-side	61	61: wire break/stretch
7	Spike detection	Function to detect spike considering the median, media and thresholds s_k in Table 4	59	59: spike if $ T3 - \text{median}(T1, T2, T3, T4, T5) \neq 0$ and $ T3 - \text{mean}(T1, T2, T3, T4, T5) > s_k$
8	High Frequency spiking	Function to identify feature in the profile like critical drops	60	60: critical drop

Deleted: Basic a
Deleted: ed

Deleted: flag

Deleted: 49: Good
50: Probably Good
51: Probably bad
52: Bad

592

593 **Gross range check**

594 The Gross range check applies a gross filter on observed temperature considering T thresholds that vary on 5
595 vertical layers, as reported in Table 3. T thresholds have been defined analyzing the seasonal T distribution in
596 4 sub-regions displayed in Figure 3: 1) the Ligurian Sea; 2) the Northern Tyrrhenian Sea; 3) the South-West
597 Tyrrhenian Sea; 4) the South-East Tyrrhenian Sea. The domain subdivision is based on the mean circulation
598 features at 15 m and 350 m depth, computed from the Mediterranean Sea reanalysis (Simoncelli et al., 2014)
599 data over the time period 1999-2018 (Figure 3). A detailed description of the circulation is out of scope here
600 but its main features are detailed in Pinardi et al. (2015) and von Schuckmann et al. (2016, section 3.1).

601 **Surface check**

602 In general, a probe needs a couple of seconds from the impact with the sea surface to stabilize its motion and
603 reach the terminal velocity (Bringas and Goni, 2015 and references therein). Different approaches have been
604 followed over the years on how to handle the near-surface values. In the late 70s, IOC proposed to extrapolate
605 upward isothermally the values from 3 to 5 m to obtain the surface temperature for encoding (IOC, 1975) while
606 the FNWC (U.S. Fleet Numerical Weather Central) procedure was to extrapolate from 8 feet (2.4 m) to the
607 surface using the slope at that depth. Wannamaker (1980) suggested reaching the surface starting from 4 m
608 using the slope between 4 and 6 m depth. Afterwards, other authors decided to discard the initial measurements,
609 considering only the values starting from a certain depth to be valid, also depending on the used DAQ (e.g.
610 Bailey et al. 1994; IOC, 1997; Kizu and Hanawa, 2002; Gronell and Wijffels, 2007; Cowley and Krummel,
611 2022 and reference therein). For example, Manzella et al. (2003) selected the value at 5 m depth as the first
612 acceptable value during MFS-PP project then changed to 4 m during MFS-TEP.

613 It is preferred that the user is provided all the original measurements by adding a test that analyzes the
614 measurements in the surface layer and annotating the resulting exit value in the ancillary variable. The
615 proposed test chooses as reference the value recorded at time t = 0.6 s (the first value currently considered
616 acceptable), calculates the differences between this value and shallower measurements and classifies them
617 using the T standard uncertainty (SD) associated to an XBT probe (0.10 °C) as a metric. In detail, the
618 temperature differences $T(t_{0.6})-T(t_i)$, with $(0.0 \leq t_i \leq 0.5)$ s are calculated and the QF is assigned as follows:

- 619 • GOOD if $|T(t_{0.6})-T(t_i)| \leq 1*SD$;
- 620 • PROBABLY GOOD if $1*SD < |T(t_{0.6})-T(t_i)| \leq 2*SD$;
- 621 • PROBABLY BAD if $2*SD < |T(t_{0.6})-T(t_i)| \leq 3*SD$;
- 622 • BAD if $|T(t_{0.6})-T(t_i)| > 3*SD$.

623 The flag GOOD means a value indistinguishable from the record at t = 0.6 s while PROBABLY GOOD defines
624 an excellent compatibility. The PROBABLY BAD and BAD flags simply indicate a difference greater than
625 the established threshold with respect to the reference value at t = 0.6 s.

626 **Inversion and gradient checks**

627 This test is performed to detect unrealistic T oscillations with abrupt T reversals or unusually large T gradients.

628 The vertical gradient is defined as the difference between vertically adjacent measurements, $T_z=(T_2-T_1)/(Z_2-$

Deleted: It

Deleted: In general, a XBT probe needs a couple of seconds from the impact with the sea surface to stabilize its motion and reach the terminal velocity (Bringas and Goni, 2015 and references therein). Different approaches have been followed over the years on how to handle the near-surface values. In the late 70s, IOC proposed to extrapolate upward isothermally the values from 3 to 5 m to obtain the surface temperature for encoding (IOC, 1975) while the FNWC (U.S. Fleet Numerical Weather Central) procedure was to extrapolate from 8 feet (2.4 m) to the surface using the slope at that depth. Wannamaker (1980) suggested reaching the surface starting from 4 m using the slope between 4 and 6 m depth. Afterwards, other authors decided to discard the initial measurements, considering only the values starting from a certain depth to be valid, also depending on the used DAQ (e.g. Bailey et al. 1994; IOC, 1997; Kizu and Hanawa, 2002; Gronell and Wijffels, 2007; Cowley and Krummel, 2022 and reference therein). For example, Manzella et al. (2003) selected the value at 5 m depth as the first acceptable value during MFS-PP project then changed to 4 m during MFS-TEP.

Deleted: The XBT measurements close to the sea surface are usually considered unreliable and thus excluded from further analysis (e.g. Bailey et al., 1994; Cowley and Krummel, 2022), due to reaching stability in motion and thermal adaptation to the surrounding environment.

Deleted: quality information

Deleted: s or quality flags

Deleted: on temperature

Deleted: ttributable

Formatted: Subscript

Formatted: Subscript

Deleted: std

Deleted: std

Formatted: Subscript

Formatted: Subscript

Formatted: Font: 11 pt

Deleted: std

Deleted: std

Formatted: Subscript

Formatted: Subscript

Deleted: std

Formatted: Subscript

Formatted: Subscript

Deleted: std

666 Z_1), where T_2 and T_1 are temperatures at depths Z_2 and Z_1 , with level 2 being deeper than level 1. This test is
 667 applied three times iteratively discarding values that failed the test in the next iteration. The acceptable T
 668 gradient ranges (Table 3) have been defined through a statistical analysis in 5 vertical layers and 4 sub-regions
 669 (Figure 3) through an approach that blends expert decisions with statistical support. Due to the spatial
 670 (horizontal and vertical) and temporal sparseness of the data, the 0.01% and 99.99% quantiles have been
 671 computed in the 5 layers considering: 1) the whole dataset; 2) the 4 sub regions; 3) the entire domain but for 4
 672 seasons. The thresholds are the absolute minimum 0.01% quantile and maximum 99.99% quantile deriving
 673 from the three cases. The thresholds of the two deepest levels are from case 1, the upper layer uses values from
 674 case 2 and the second and third layers use the results of case 3.

675 **Table 3 Temperature and thermal gradient thresholds defined in 5 layers.**

Layer	Temperature (°C)		Vertical Gradient (°Cm ⁻¹)	
0-100 m	12.000	30.000	-3.400	0.613
100-250 m	12.500	17.900	-0.317	0.244
250-450 m	12.700	15.500	-0.156	0.170
450-1000 m	13.100	14.800	-0.133	0.137
1000-2300 m	13.100	14.000	-0.094	0.090

676
 677 **Wire break/stretch**
 678 Results of inversion and gradient checks are used to identify sharp variations toward negative values, indicating
 679 that the copper wire breaks on shipside, or toward high values (close to 35 °C or more), when the wire breaks
 680 on probe-side where there is often a progressive increase in temperature values rather than a step transition to
 681 full scale.

682 **Spike detection**
 683 This test looks for single value spikes and it checks T measurements for large differences between adjacent
 684 values. A spike is detected by computing the median value (Med_k) in a 5 points interval (3 m approximately)
 685 with the profile value at the central point of the interval (T_k). The spike is detected and the consequent flag is
 686 applied if T_k is not equal to Med_k and the difference (s_k) between T_k and the mean (Ave_k) in the chosen
 687 interval is greater than a threshold value.

$$688 \quad Med_k = median(T_{k-2}:T_{k+2})$$

$$689 \quad Ave_k = mean(T_{k-2}:T_{k+2})$$

$$690 \quad s_k = T_k - Ave_k, \quad c_k = T_k - Med_k \neq 0$$

691 The spike threshold values have been defined for the entire region in 5 vertical layers as the 99.9% quantile of
 692 the s_k distribution and they are reported in Table 4. Figure 4a shows the probability distribution of s_k values
 693 with c_k not equal to zero in 5 layers. s_k distribution is characterized by large values above 80 m that diminish

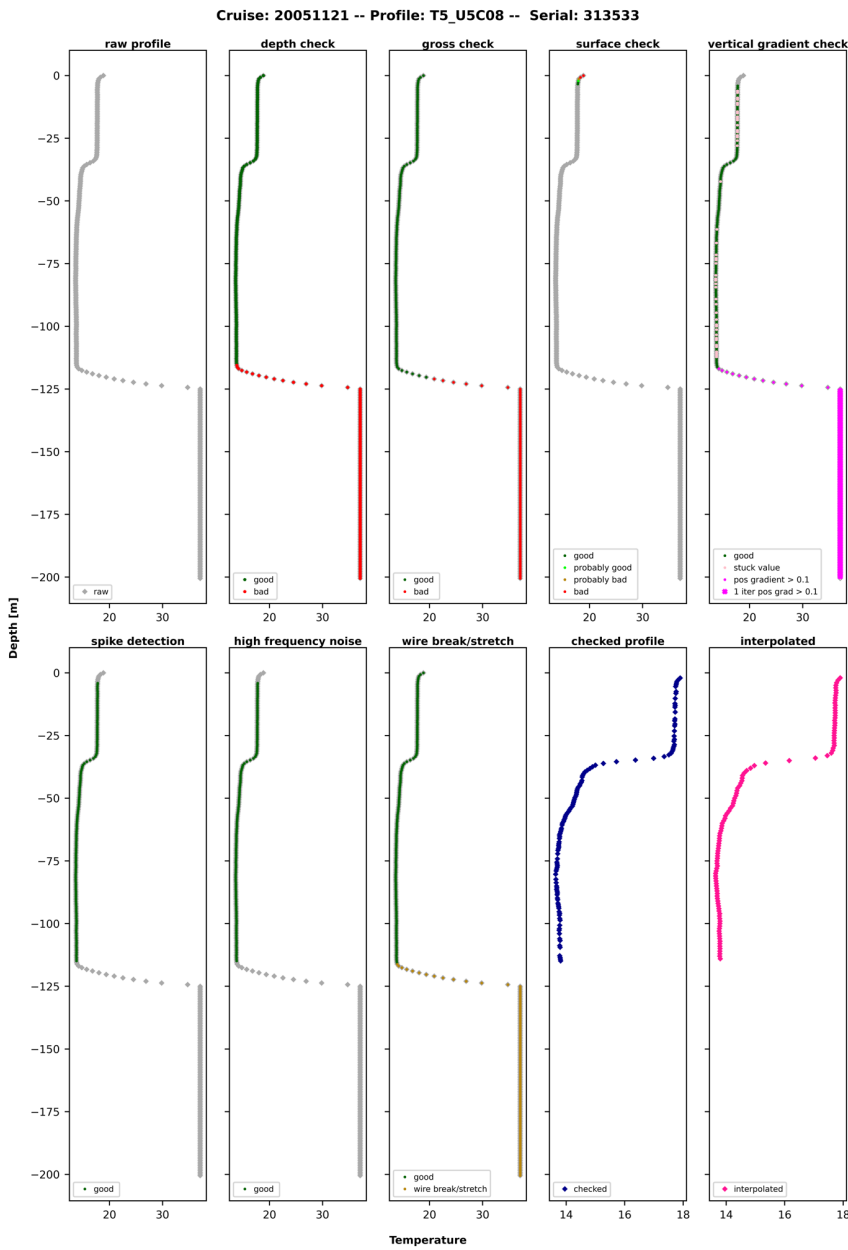
Deleted: 3a

695 with depth, as the temperature variability does. The s_k scatter plot (Figure 3b) shows its values along the water
696 column, with the red dots highlighting the values over the selected thresholds.

697 **Table 4 Spike detection threshold defined in 5 vertical layers.**

Layer	spike threshold (°C)
0-80 m	0.236
80-200 m	0.085
200-450 m	0.054
450-900 m	0.050
900-2300 m	0.022

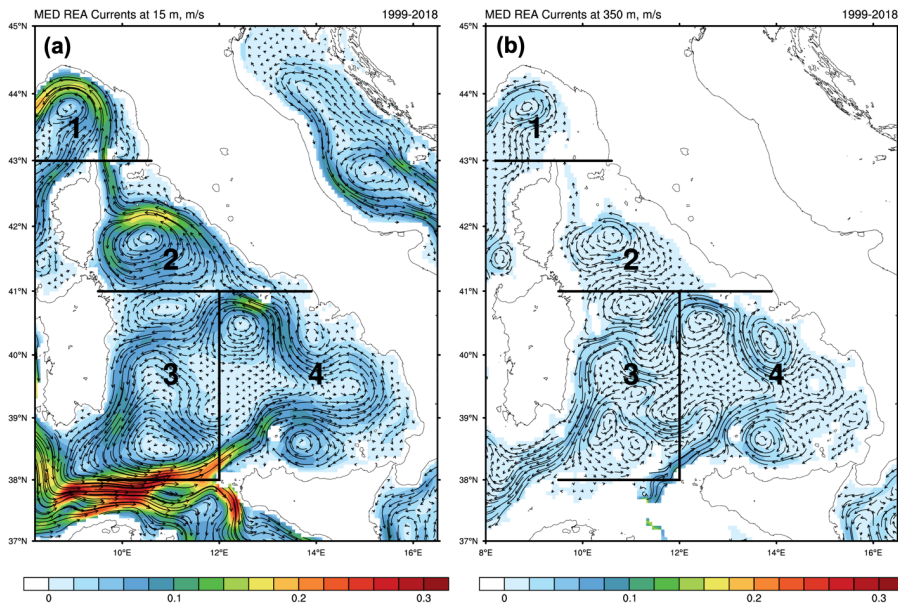
698
699 **High Frequency Noise**
700 It helps to identify critical T drops in the profile (such as large T differences over a large depth) by checking
701 continual spiking over a wide range of depths (Cowley and Krummel, 2022). In case of continual spikes, values
702 before and after a chosen interval (4 m approximately, i.e. 7 points) are tested considering the same acceptable
703 range of T inversion and gradient as in the *inversion and gradient checks* and flagged as bad if they are out of
704 the ranges.



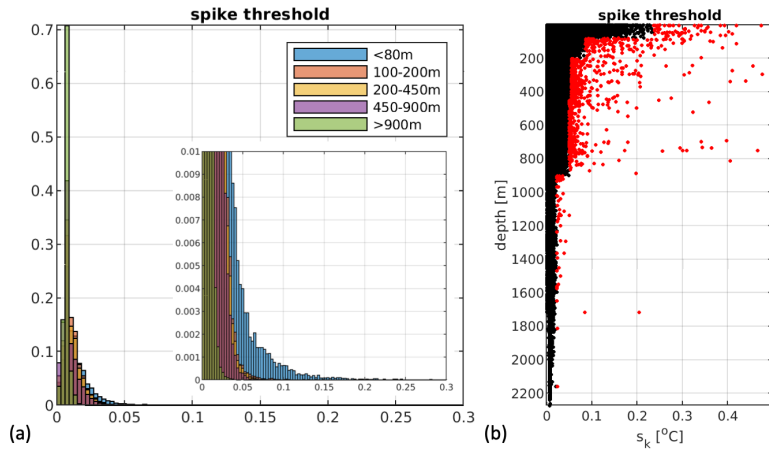
705

706 Figure 2 Example of the **QEs** generated by the automatic QC tests (Table 2) applied to a temperature profile. The
 707 raw profile is at the top left and the final interpolated profile is at the bottom right.

Deleted: quality flag



709
 710 Figure 3 Maps of the mean circulation computed from the Mediterranean Sea reanalysis dataset (Simoncelli et al.,
 711 2014) at (a) 15 m and (b) 350 m depth.



712
 713 Figure 4 (a) Distribution in terms of probability of the spike threshold (s_k) in 5 layers with a zoom probability
 714 below 0.1%. (b) Vertical distribution of the spike threshold with indication in red of the values above the 99.99%
 715 quantile.

716 **4.2 Mapping QC test exit values to standard Quality Flags**

Deleted: outcome

717 Each basic QC test assigns a corresponding exit value to each original depth (DEPTH_TEST_QC) and T
718 (TEMPET01_TEST_QC) record (Table 3) within the vertical profile and their mapping to QFs is necessary to
719 allow the user to filter the original data according to the quality requirements for the intended use. The QFs
720 adopted, whose labels and corresponding definition are reported in Table 5, have been selected from the SDN
721 Common Vocabulary (IOC, 2013; IOC, 2019; <https://www.seadatanet.org/Standards/Common-Vocabularies>).
722 The QF (Table 5) associated with each original T measurement or depth value summarizes the results of the
723 performed automatic tests and it is stored in the dedicated ancillary variable (TEMPET01_FLAGS_QC or
724 DEPTH_FLAGS_QC).

Deleted: or label

725 **Table 5 The Quality Flags (QF) selected from the SeaDataNet Common Vocabulary (IOC, 2013; IOC, 2019)**
726 **assigned to the reprocessed XBT data.**

Deleted: /UNESCO

id	label	definition
1	good value	Good quality data value that is not part of any identified malfunction and has been verified as consistent with real phenomena during the quality control process
2	probably good value	Data value that is probably consistent with real phenomena but this is unconfirmed or data value forming part of a malfunction that is considered too small to affect the overall quality of the data object of which it is a part
3	probably bad value	Data value recognised as unusual during quality control that forms part of a feature that is probably inconsistent with real phenomena
4	bad value	An obviously erroneous data value
8	interpolated value	This value has been derived by interpolation from other values in the data object.

727
728 The general rule adopted for both depth and T QF is the following:

- 729 • GOOD (QF=1) where all the tests pass;
- 730 • BAD (QF=4) where at least one of the checks fails.

731 For T, we decided to use a higher level of detail, introducing also “probably good” (QF=2) and “probably bad”
732 (QF=3) flags, when it’s needed, since surface and inversion/gradient tests can provide more information on
733 profile behavior. After applying general rule for GOOD and BAD flags, we consider the flags coming from
734 the two mentioned tests and we update the flags as follows:

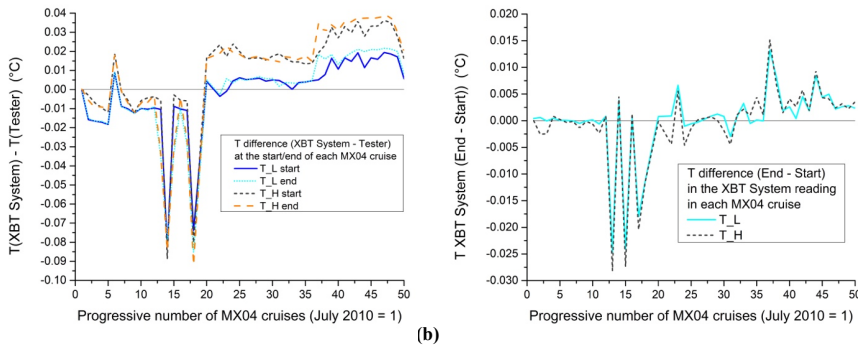
- 735 • PROBABLY GOOD (QF=2) if the surface test returns a “probably good” flag;
- 736 • PROBABLY BAD (QF=3) if the surface and/or the inversion test returns a “probably bad” flag.

737 Only measurements that have associated T and depth QFs equal to 1 or 2 have been used for the interpolation
738 at each meter depth. A relative QF associated to the interpolated profile has also been generated in order to
739 label (“interpolated value”, QF=8) when there is a gap of more than 5 consecutive points in the original profile,
740 which coincides with the number of points used to detect spikes (~3 m).

744 **4.3 Calibration of the XBT system and correction**

745 As previously highlighted, checking with a tester provides an assessment of the efficiency of an XBT system.
 746 Once a tester is connected to an XBT system in a simulated drop, the tester's measurement indicates how the
 747 XBT system's reading differs from nominal values at some reference temperatures. These differences, which
 748 can be constant or variable over the time interval of data acquisition, can then be used to correct the values of
 749 the XBT profiles. Each tester used during the campaigns on the MX04 line after July 2010 has two reference
 750 temperatures (see Appendix A for details).
 751 Checks, immediately before the first drop and after the last drop, were routinely performed. Further checks
 752 were carried out whenever the computer or DAQ had failures. The differences measured at the reference
 753 temperatures at the start/end of each MX04 cruise are shown in Figure 5a, while their drift during a cruise is
 754 shown in Figure 5b. The values vary marginally and slightly over the time, but large anomalies occurred in
 755 September 2013 (cruise 14) and June 2014 (cruise 18) for unknown reasons. The DAQ used in those campaigns
 756 showed an initial offset followed by a random and oscillating variability throughout the day: for example, the
 757 recorded values during the checks in June 2014 were 26.678 °C (start), 26.649 °C, 26.668 °C and 26.666 °C
 758 (end) instead of 26.758 °C. This type of anomaly was also found from Reseghetti et al. (2018) during XBT vs.
 759 CTD comparison tests, where it was pointed out that the T differences between the XBT and CTD profiles
 760 were heavily affected by the DAQ functioning.

- Deleted: For example, Reseghetti et al. (2018) showed a notable improvement in the accuracy of XBT values compared to measurements from a reference instrument (a CTD) in dedicated field tests when tester control correction was applied.
- Deleted: The testers used here (built with high-performance resistors) have two reference temperatures (see Appendix A for details).
- Deleted: reading
- Deleted: both
- Deleted: The performance of the XBT system used was verified only for some subsets of the REP dataset. Since July 2010, a two-point tester has been used during cruises on the MX04 line with an initial
- Deleted: c
- Deleted: drop
- Deleted: a final one
- Deleted: profile
- Deleted: . Additional checks were performed
- Deleted: s
- Deleted: It is well evident that t
- Deleted: only
- Deleted: large anomalies occurred



762 (a) (b)
 763 **Figure 5 (a) Temperature difference (XBT System-Tester) obtained from the checks at the reference temperatures**
 764 **before starting and at the end of each MX04 cruise. (b) Difference between initial and final measurement with the**
 765 **tester during the same cruise at the reference temperatures.**

766 **4.3.1 Correction Algorithm**

767 The measurements with a tester are used to correct the T values of each XBT profile of a campaign under the
 768 assumption that the difference between the initial and final tester readings at reference temperatures varies
 769 linearly over time from the beginning to the end of the campaign. The reference values are obtained by
 770 calculating the average resistance value over the last 30 consecutive recorded values at each temperature in

794 the simulated drop (i.e. 3 seconds of acquisition, with a sampling frequency of 10 Hz) and then converted into
 795 T values (for details, see Appendix A). The differences between the nominal temperatures and the read values
 796 are linearly interpolated as a function of the time elapsed since the first launch to calculate their hypothetical
 797 value in correspondence with each XBT probe during the campaign. In case of a single-point tester, a constant
 798 correction is added to each value of the XBT profile. In case of two-point tester, the correction is obtained by
 799 a further linear interpolation, based on the differences at upper and lower temperatures of this tester.

800 Notation:

- 801 • N is the number of XBT probes deployed during the campaign;
- 802 • T_+ and T_- nominal upper and lower temperature on the tester;
- 803 • $\Delta T_{+,i}$, $\Delta T_{+,f}$ initial and final temperature difference at the value T_+ ;
- 804 • $\Delta T_{-,i}$, $\Delta T_{-,f}$ initial and final temperature difference at the value T_- ;
- 805 • t_i , t_f initial and final time of the XBT drops (usually, t_i is set to 0);
- 806 • t_k time elapsed from the initial check with the tester, which is assumed to be coincident with the first
 807 XBT drop ($1 \leq k \leq N$);
- 808 • $T_{+,k}$ and $T_{-,k}$ theoretical upper and lower temperature that the tester should read at the k-th drop.

809 These last values can be calculated as

$$810 T_{+,k} = T_{+,i} + \Delta T_{+,k} \quad \text{and} \quad T_{-,k} = T_{-,i} + \Delta T_{-,k}$$

811 where the estimated difference at upper and lower reference T corresponding at the k drop are:

$$812 \Delta T_{+,k} = - \left[\Delta T_{+,i} + \left(\frac{\Delta T_{+,f} - \Delta T_{+,i}}{t_f - t_i} \right) (t_k - t_i) \right] \quad \text{and} \quad \Delta T_{-,k} = - \left[\Delta T_{-,i} + \left(\frac{\Delta T_{-,f} - \Delta T_{-,i}}{t_f - t_i} \right) (t_k - t_i) \right]$$

813 The so calculated contributions are combined in the correction term for the specific k XBT:

$$814 \Delta T_{corr,k} = \left(\frac{\Delta T_{+,k} - \Delta T_{-,k}}{T_+ - T_-} \right) (T_{read,k} - T_-) + \Delta T_{-,k}$$

815 and then added the original value $T_{read,k}$ recorded by the DAQ:

$$816 T_{corr,k} = T_{read,k} + \Delta T_{corr,k}$$

817 $T_{corr,k}$ is thus the value that best represents the actual seawater temperature measured by the k XBT probe
 818 assuming that the calculated correction (based on the initial and final measurements provided by the tester) is
 819 the best way to describe how the XBT system operates when the probe was deployed. Obviously, $\Delta T_{corr,k}$ is not
 820 related to the measurement quality due to the probe characteristics or to possible issues during data acquisition.

821 When the calibration is available, the correction calculated in this way has been applied to the raw data prior
 822 to the QC analysis but it is also provided as a separate variable (**CALIB**) so that the user might decide to
 823 remove it. This correction must absolutely not be applied to the profiles from XCTD-1 probes because their
 824 acquisition circuit works in a completely different way and the shipboard DAQ simply acts as a data receiver
 825 and does not play an active role in the measurement.

Deleted: the k-th

Deleted: k-th

Deleted: k-th

Deleted: ; while i

Deleted: i-th

Formatted: Font: Italic

Deleted: -th

Formatted: Font: Italic

Deleted: -th

Deleted: k-th

Deleted:

Deleted: crossing the water column and measuring

Deleted: cannot say anything about

Deleted: the quality of

Deleted: of the k-th probe ("hot" or "cold" probe,

Deleted: troubles

Deleted: the

Deleted:)

842 **4.4 Vertical interpolation**

843 Three interpolation methods were tested: linear (LI), RR (Reiniger and Ross, 1968) and MR-PCHIP (Barker
844 and McDougall, 2020). The goal is to select the most conservative method, i.e. the one that provides the closest
845 interpolated T values to the original reading. The original measurements of each XBT profile were subsampled,
846 discarding half of the measurements then used as control values against the newly interpolated ones to calculate
847 differences and Root Mean Square Differences (RMSD) and therefore evaluate the best interpolation method
848 for our dataset.

849 Original values have been interpolated with the three methods on the control depth levels and the resulting T
850 estimates have been compared with the measured ones. Figure 6 shows an example of an observed profile with
851 highlighted control levels (magenta), the interpolated profile with the three considered methods and the relative
852 differences (interpolated-original). Figure 6a presents an example of the large T differences that occur between
853 interpolated and measured values (0.4 °C or -0.2 °C) along the thermocline at about 35 m. Figure 6b shows a
854 step-like profile below 600 m depth where the differences are very small, less than 0.02 °C, but they can
855 slightly increase and differ among the three methods where T vertical gradients occur.

856 Mean bias and RMSD have been computed in vertical bins (766) of 3 m thickness and the obtained metrics
857 profiles are displayed in Figure 7, associated with their relative vertical data distributions. These metrics have
858 been computed for the whole dataset and for two separate time periods: from June to November (when the
859 thermocline is well developed) and from December to May (when the water column is more homogeneous).
860 The mean bias in Figure 7 presents values in the range (-0.001, +0.001) °C, the interval halves from December
861 to May whereas it practically doubles (-0.002, +0.001) °C from June to November. The maximum RMSD
862 when considering all profiles is about 0.04 °C, it halves from December to May while it is close to 0.06 °C
863 from June to November. Except for the ~~Dec-May~~ plot, the maximum RMSD values are associated with LI and
864 RR methods but we note that $RMSD < 0.01$ °C for the three methods below 100 m depth.

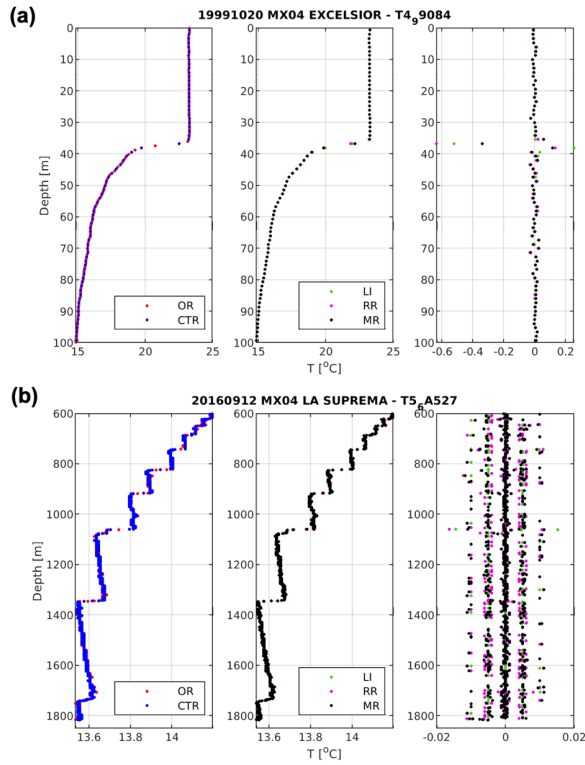
865 The total RMSD on the entire water column has been summarized in Table 6 for the three time periods and
866 the surface layer above 100 m. In fact, the total bias estimated is zero for the three methods and the three time
867 periods, while the total RMSD is 0.011 °C for LI, 0.011 °C for RR and 0.010 °C for MR-PCHIP, while in the
868 surface layer the values are 0.023 °C, 0.021 °C and 0.019 °C respectively. The maximum RMSD values usually
869 occur during the stratified period (Jun-Nov) with values equal to 0.013 °C for LI, 0.012 °C for RR and 0.011
870 °C for MR-PCHIP, that in the surface layer become 0.030 °C, 0.027 °C and 0.023 °C, respectively.

871 The computed metrics in vertical bins present very small values, much lower than ~~and the specified T~~
872 ~~uncertainty (0.10 °C)~~. However, the absolute differences in the surface layer when the thermocline settles can
873 be larger than 0.2 °C as in Figure 6. The MR-PCHIP interpolation always presents the smallest error for the
874 analyzed dataset (Table 6) with respect to the reference values, thus it has been applied.

Deleted: "mixed"

Deleted: the nominal accuracy associated with the measurements of an XBT system (0.2 °C)

Deleted: to the REP dataset

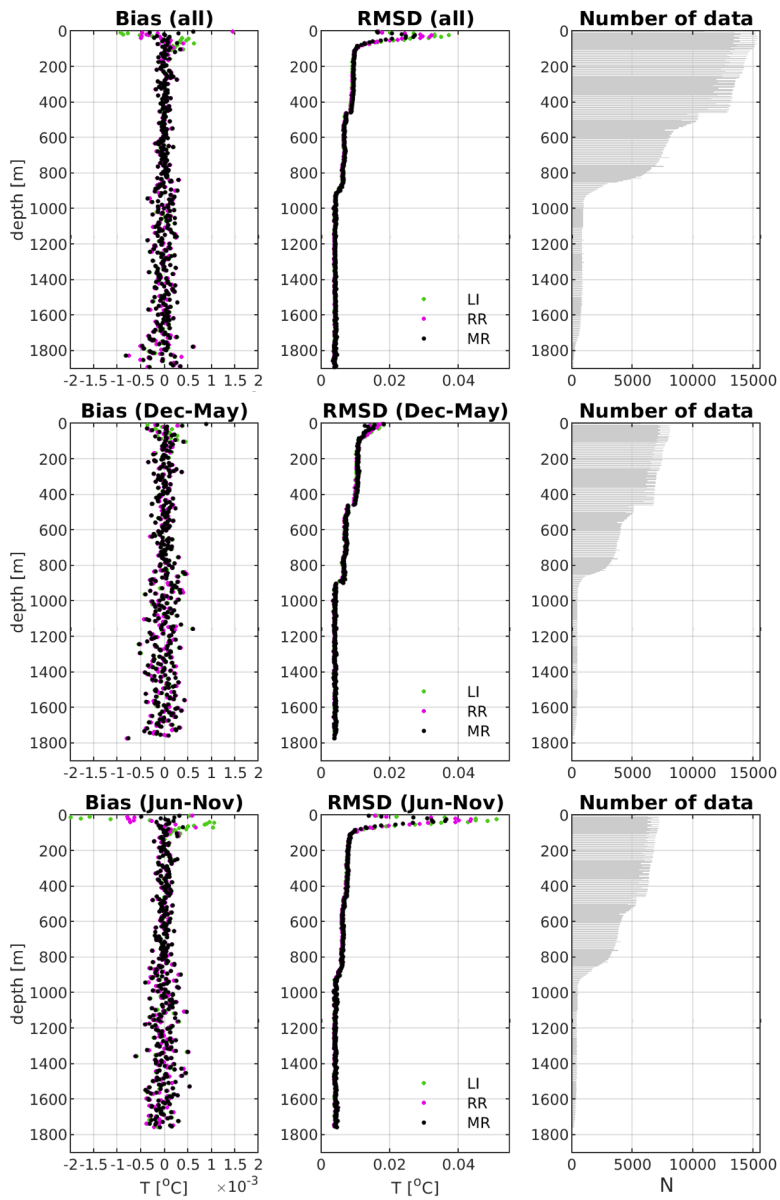


879

880 **Figure 6** Temperature profiles in the surface layer 1-100 m (a) and in the deep layer 600-1800 m (b): (left) magenta
 881 dots represent the control records; (middle) interpolated temperature values with linear LI (linear) , RR (Reiniger
 882 and Ross, 1968) and MR-PCHIP (Barker and McDougall, 2020); (right) differences between the interpolated and
 883 measured T values.

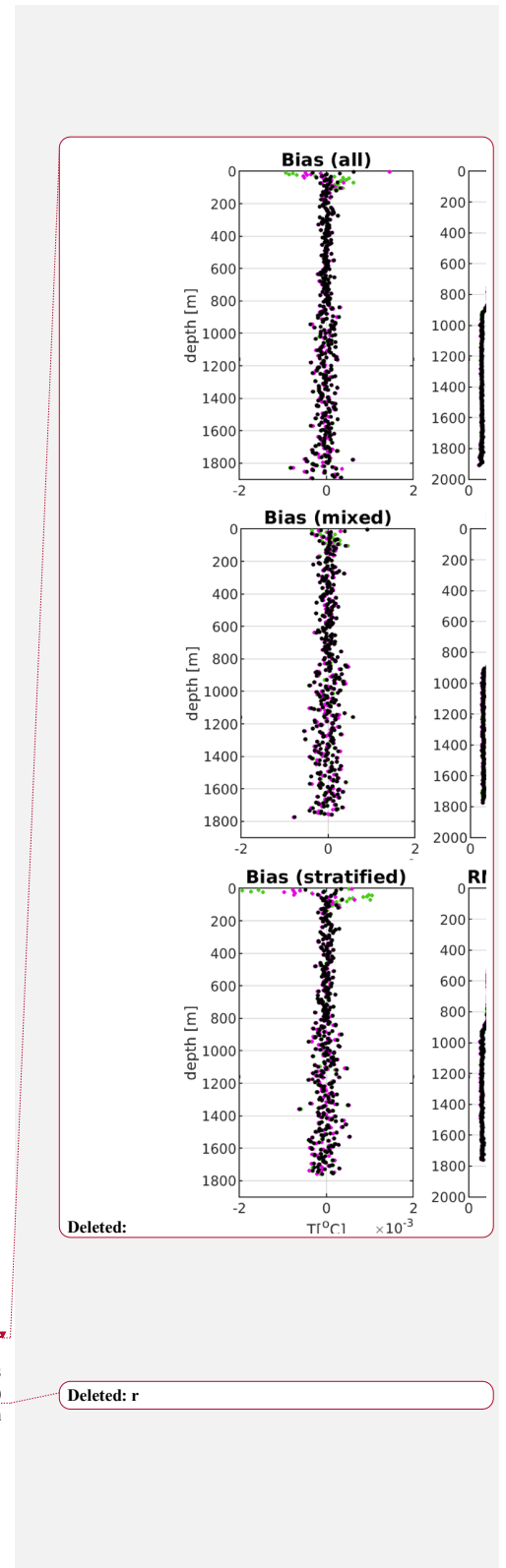
884 **Table 6** Summary of the computed metrics from the three interpolation methods: linear (LI), RR and MR-PCHIP
 885 Temperature RMSD [°C] have been computed in the entire water column and in the surface layer (0-100 m) from
 886 the whole dataset (All) and in two time periods December-May (mixed) and June-November (stratified).

RMSD	LI	RR	MR-PCHIP
All	0.011	0.011	0.010
0-100 m	0.023	0.021	0.019
Dec-May	0.010	0.010	0.010
0-100 m	0.014	0.014	0.013
Jun-Nov	0.013	0.012	0.011
0-100 m	0.030	0.027	0.023



887

888 Figure 7 Profile of mean bias (left) and RMSD (middle) computed from profiles interpolated on selected depths
 889 and compared to the corresponding measured values considering the three methods: linear (LI), MR-PCHIP (MR)
 890 and Reniger and Ross (RR). Three different time spans are shown: (top) the whole dataset; (middle) from
 891 December to May; (bottom) from June to November. (right) Vertical data distribution in 3 m bins.



Deleted: r

894 **5. Results**

895 ~~The QC algorithms applied to the dataset are not capable of catching all erroneous values.~~ According to Good
896 et al. (2023) any automatic QC test produces a percentage of True Positives (TP, correctly detected erroneous
897 data) and False Positives (FP, incorrectly detected erroneous data) and the general aim would be to maximize
898 the TP (correct flagging) rate and minimize the FP (incorrect flagging) rate.

899 The new automatic QC procedure has been ~~tuned using visual checks~~ to reach an optimal TP/FP rate.
900 ~~Specifically,~~ efforts have been made to tune the vertical gradient and spike thresholds, ~~using~~ quantiles analysis
901 to maximize the detection of erroneous data (TP) and minimize ~~flagging of GOOD data as BAD (FP)~~. This
902 was particularly tricky for the vertical gradient test which detected 121 profiles with out of bounds values, but
903 28 of them appeared FPs (FP/TP rate of 23%) from visual check. In fact, the strong seasonal stratification of
904 the Mediterranean Sea and the presence of several water masses in different water layers might cause the
905 incorrect flagging of GOOD data ~~as BAD (FP)~~, as shown in Figure 8b,d. This makes the vertical gradient test
906 non-optimal for the Mediterranean Basin with a high FP rate, thus a very small percentage associated with the
907 quantiles have been selected to minimize this.

908 The spikes test ~~is~~ much more effective (331 profiles with detected spikes of which 11 are FPs), providing a
909 low FP/TP rate (3.3%). Figure 9 shows example profiles with ~~TP~~ spikes (a) and ~~FP~~ spikes (b), mainly marked
910 at the start of the thermocline.

911 However, some profiles present anomalous features that automatic QC procedure could not detect. The
912 decision was to add a flag associated with the whole profile indicating the depth range where unrecoverable
913 problems began. ~~The decision is based on~~ the knowledge of the main physical characteristics of the water
914 masses present in the analyzed region. In fact, the very small ~~Rosby radius (~11 km on average)~~ and the
915 occurrence of repeated and well-documented thermal inversions must always be considered when the quality
916 of the T profiles is analyzed. Step-like structures (“staircases”) are also typical of the southern Tyrrhenian Sea,
917 explained usually in terms of the double diffusion process (Meccia et al. 2016; Durante et al., 2021).

918 Sometimes, the meteorological conditions and a non-accurate knowledge of the bathymetry can make the
919 expert validation of XBT profiles difficult, but their extreme variability can also be ascribed to multiple
920 instrumental and operational factors. In every XBT drop, the correct unwinding of the wire from both spools,
921 adequate and complete protection of the insulating substance along its entire length are essential to guarantee
922 good quality of the recorded data. For example, most profiles from XBTs launched from ships traveling at low
923 speed (i.e. $v < 15$ knots, ~~less than 10% of the dataset~~) are generally less affected by significant electrical
924 disturbances, even in the presence of ~~wind~~. Unfortunately, the ships used on the MX04 line (from which most
925 of the REP profiles belong) have a standard speed close to 22 knots and this makes the acquisition conditions
926 vulnerable. The XBT profiles from containerships also have a lower quality due to the usually very high launch
927 position ($h > 25$ m), which ~~makes the probe depth in the initial measurements provided by software~~
928 questionable (Bringas and Goni, 2015). ~~As mentioned in section 2,~~ the electric current ~~that circulates in the~~
929 ~~unwinding~~ copper wire ~~transforms it into~~ an antenna sensitive to all electromagnetic phenomena occurring in
930 ~~nearby~~. The occurrence of atmospheric events (thunderstorms with lightning) can have a non-negligible impact

Deleted: The application of a series of QC algorithms to detect erroneous values is not capable of catching all of them

Deleted: deeply

Deleted: by

Deleted: In

Deleted: s

Deleted: tuned by

Deleted: ,

Deleted: to flag as

Deleted: BAD

Deleted: the GOOD ones

Deleted: as BAD

Deleted: instead

Deleted: true

Deleted: wrong

Deleted: indispensable premise is

Deleted: value of the

Deleted: \leq

Deleted: 5

Deleted: irregardless of the season

Deleted: non-zero

Deleted: also

Deleted: n XBT, during acquisition, due to

Deleted: present

Deleted: , acts as

Deleted: in the atmosphere

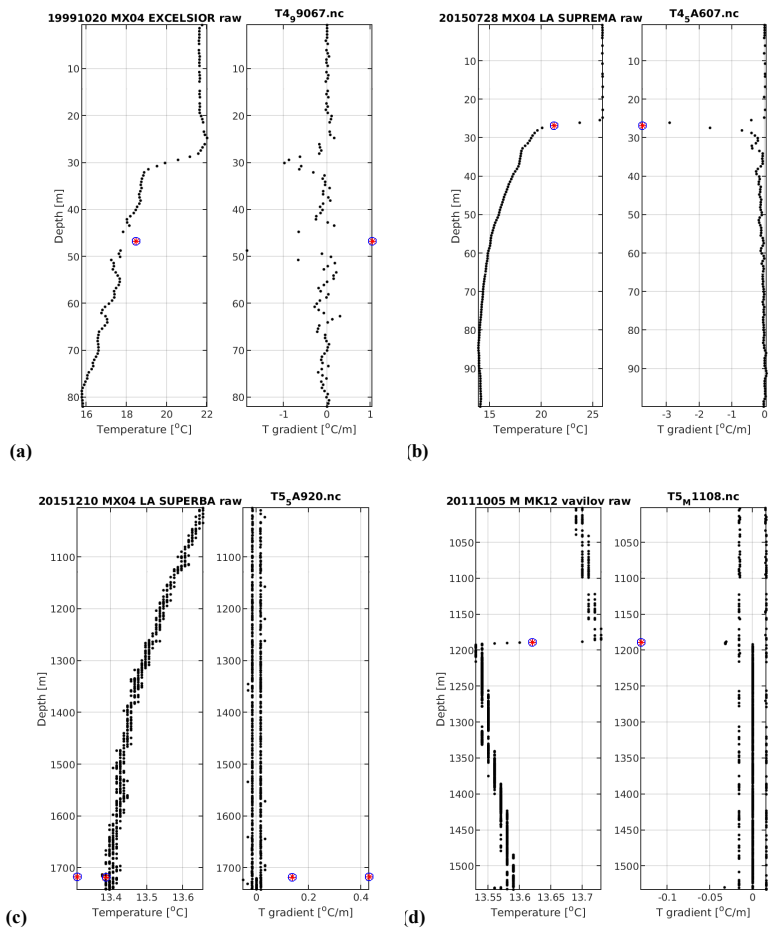
Deleted: a

Deleted: region close to the launching position and on the ship

Deleted: , even at a relative distance from the ship,

961 on the recorded signal, same as the proximity to on-board instrumentation producing significant
 962 electromagnetic fields and whose operation is random. The physical parameter measured by the XBT system
 963 is the electrical resistance, which has two components: one is from the copper wire and the other from the NTC
 964 thermistor which falls through the water column. Gusts of wind combined with turbulence produced by the
 965 ship hull can produce "whiplash" on the copper wire and badly influence the shape of the profiles collected
 966 with particularly unfavorable wind conditions.

Deleted: the "cleanliness" of

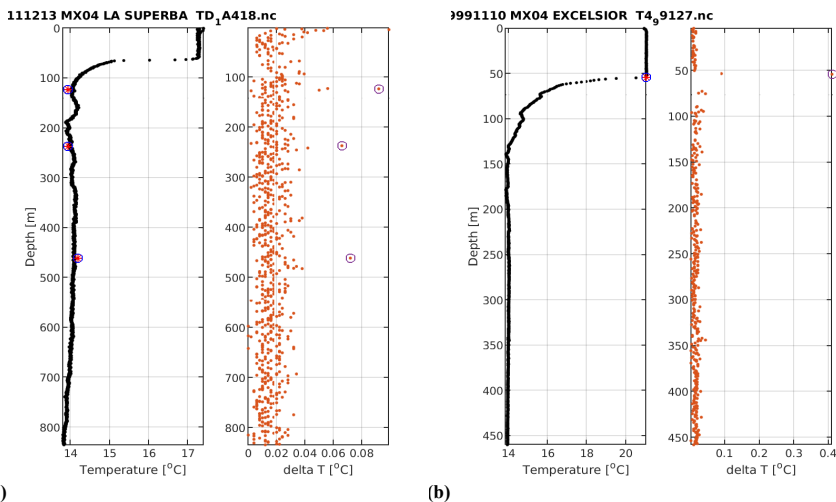


967

968

969 Figure 8 Examples of temperature gradient flags applied to different XBT profiles: (a) true positive vertical
 970 gradient anomaly in the surface layer; (b) false positive vertical gradient anomaly in the surface layer; (c) true
 971 positive vertical gradient anomaly in the bottom layer; (d) false positive vertical gradient anomaly in the bottom
 972 layer. The sub-plots have different axes ranges.

Deleted: true



975

(a)

(b)

976 **Figure 9** Examples of spikes detected in two different XBT profiles: (a) true **positive** spikes; (b) false **positive** spike
 977 at the start of a steep thermocline. The orange dots in the right panels of (a) and (b) indicate the estimated value
 978 of the s_k parameter having c_k not equal to zero. **The sub-plots have different axes ranges.**

979 A difficult task has been how to identify the external influences that **cause high frequency noise** in the T profile,
 980 as in the examples of Figure 10 c-d-e, and how to annotate it in the metadata. Some other anomalous thermal
 981 structures, compared to what is expected in a certain period, region and depth layer are shown in Figure 10 a-
 982 b and f (anomaly around 400 m depth in the blue profile and at 550 m in the green one). The visual check
 983 carried out by the expert allows in some cases to highlight notable deviations in the shape and/or values of a
 984 profile compared to adjacent ones. The probability of having the same type of anomalous structure recorded
 985 by two adjacent XBT probes in time and space is considered negligible, favoring the occurrence of something
 986 physical, instead of non-optimal functioning of a specific probe. Sometimes the initial BAD attribution to
 987 anomalous structures was subsequently reviewed by the comparison with adjacent profiles that present similar
 988 features (e.g. Fig. 10 a).

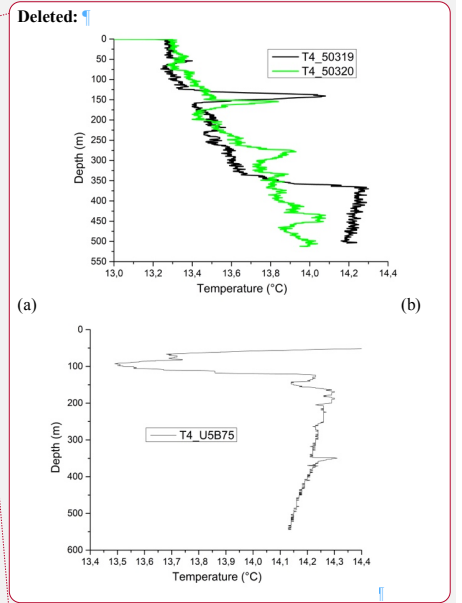
989 5.1 Comparison with SeaDataNet data version

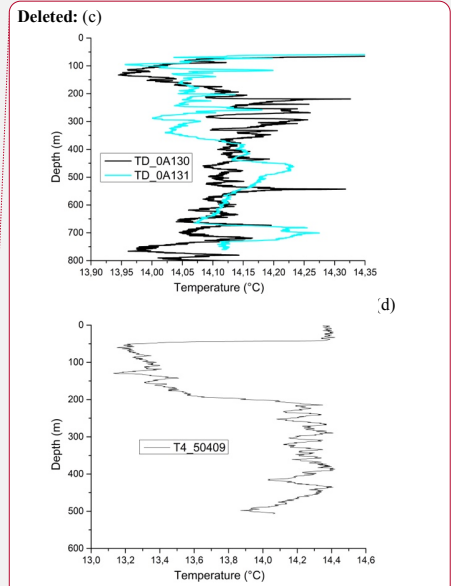
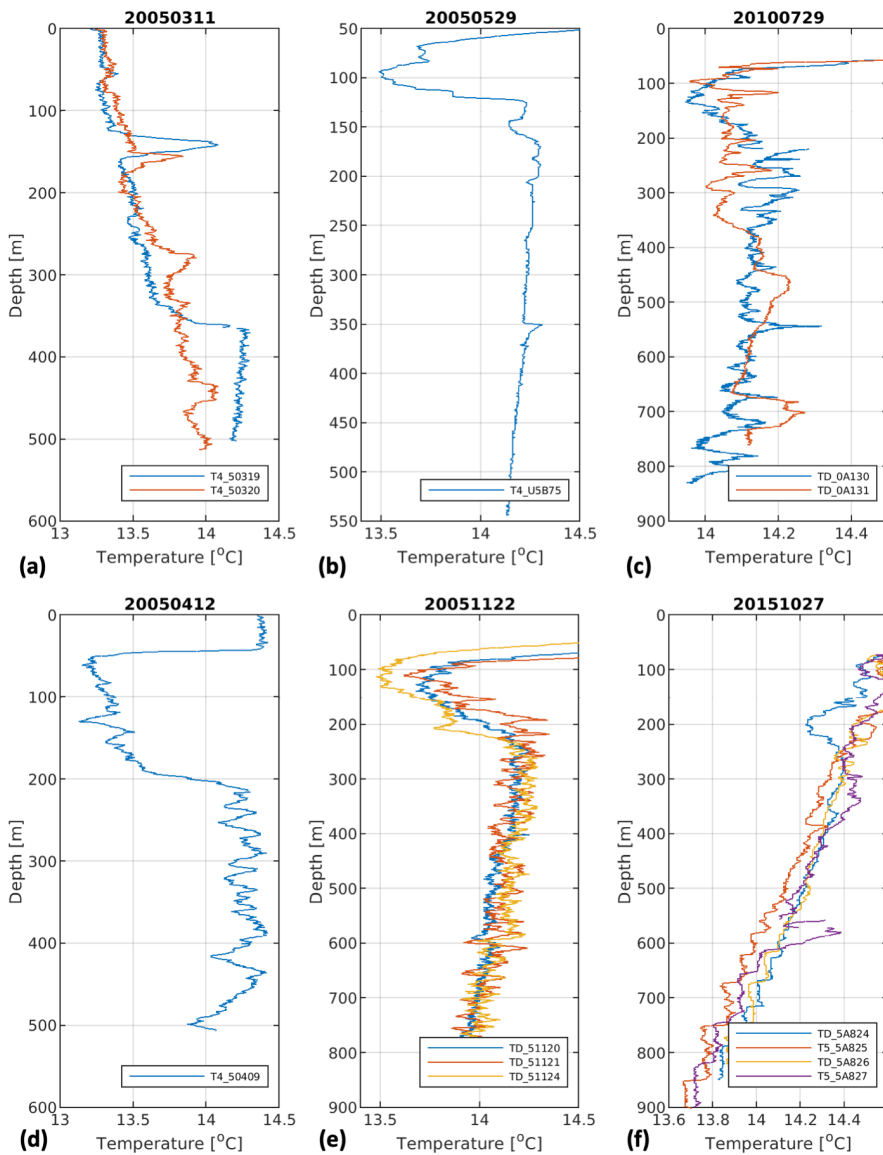
990 A significant part of the XBT profiles included in this dataset have been systematically disseminated through
 991 the SDN infrastructure and can be accessed from the data access portal through the saved query Url
 992 https://cdi.seadatanet.org/search/welcome.php?query=1866&query_code={4E510DE6-CB22-47D5-B221-7275100CAB7F}.
 993 Alternatively, they can be found in the Mediterranean aggregated dataset product
 994 (Simoncelli et al., 2020a) in which they are integrated with other data types (CTDs, bottles, MBTs, profiling
 995 floats). This data product has been further validated in the framework of the SeaDataCloud project
 996 (<https://www.seadatanet.org/About-us/SeaDataCloud>), as described in Simoncelli et al. (2020b).

- Deleted: se
- Deleted: induce "oscillations"
- Deleted: shape of
- Deleted: "
- Deleted: something
- Deleted: Validation

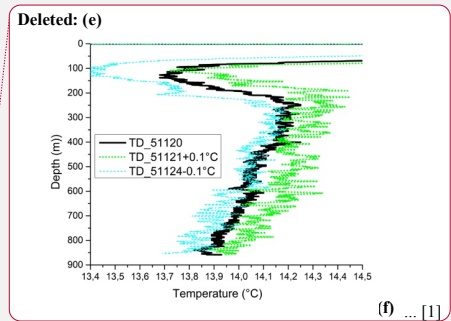
1012 The SDN XBT dataset, extracted from Simoncelli et al. (2020a) is considered here as a benchmark to highlight
1013 the main effects of the proposed data reprocessing. Bias and RMSD profiles have been computed from 3104
1014 matching profiles with a vertical data distribution shown in Figure 11. Since SDN profiles do not have the
1015 calibration correction, we have computed the separate metrics with and without the correction applied. The
1016 black dots represent all matching profiles, green dots represent the profiles without correction and the red dots
1017 have the correction applied.

Formatted: Justified, Border: Top: (No border), Bottom: (No border), Left: (No border), Right: (No border), Between : (No border)





Formatted: Font: Not Bold
Formatted: Justified



Moved (insertion) [1]
Deleted: (
Deleted:)
Deleted: Remark: t
Deleted: are different and selected to highlight some peculiar structure
Deleted:
Moved up [1]: The name of the selected profile(s) is shown in the legend.

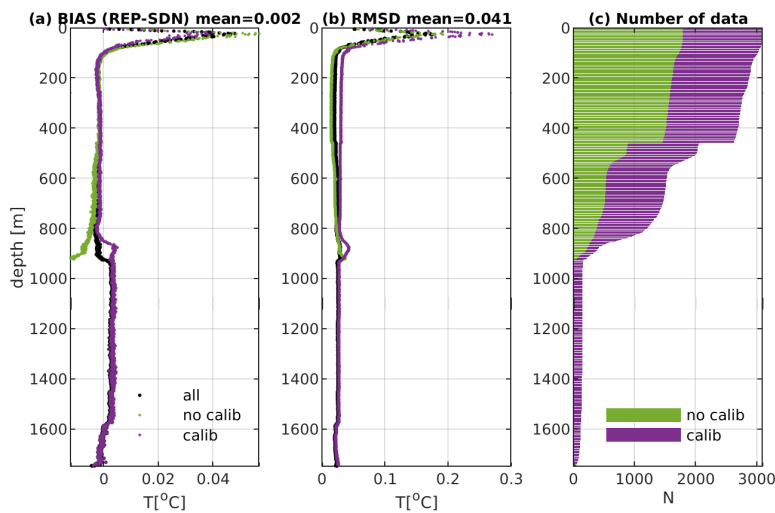
1021

1022

1023

Figure 10 Examples of profiles with critical features. The name of the selected profiles is shown in the legend. The sub-plots have different axes ranges.

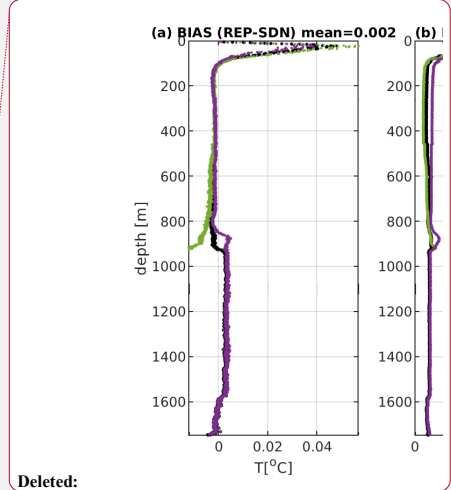
1040 The maximum discrepancy among the two data versions resides always within the surface layer until 150 m
 1041 depth. The maximum bias and RMSD reach approximately 0.05 °C and 0.2 °C respectively, which might imply
 1042 potential significant changes in downstream applications. The bias is larger (~0.06 °C) when estimated from
 1043 profiles without calibration correction and slightly smaller (~0.04 °C) from calibrated profiles, while the largest
 1044 RMSD derives from profiles with the correction applied, indicating that the correction slightly increases on
 1045 average the REP temperature values and consequently the positive bias.
 1046 The REP profiles are warmer than SDN ones in the surface layer and below 900 m, while between 150 m and
 1047 800 m both metrics are small and consistent. The overall mean bias and RMSD are equal to 0.002 °C and 0.041
 1048 °C, respectively. Such differences are mainly due to the new interpolation technique, the lack of filtering, the
 1049 application of the calibration correction in the REP dataset, and in very few cases, the use in SDN of wrong
 1050 FRE coefficients or the incorrect probe type assignment which can produce a change of the depth values. The
 1051 sharp reduction in the number of observations available below about 900 m depth and the application of the
 1052 tester correction affect the shape of both BIAS and RMSD profiles.



Deleted: non-correc

Deleted: quite constant

Deleted: The sharp reduction in the number of observations available below about 900 m depth could affect the shape of both BIAS and RMSD profiles.



Deleted:

1054 **Figure 11 Comparison between the reprocessed (REP) and the corresponding SeaDataNet (SDN) profiles at each**
 1055 **meter depth: (a) Bias mean profile; (b) RMSD profile and (c) cumulative vertical data distribution which shows**
 1056 **the relative contribution of profiles with calibration and profiles without calibration to the total.**

1057 Figure 12 shows examples of matching REP and SDN profiles and their difference with a zoom in the surface
 1058 (a) and bottom layer (b and c), where the largest differences occur. During the stratified period, the largest
 1059 differences reside in the thermocline and can exceed 1.5 °C (Figure 12a), while in the bottom layer the
 1060 calibration correction (see Figure 12b, c) together with the abrupt decrease of the number of data explain the
 1061 small positive average bias in Figure 11a. In fact, numerous T5/20 profiles (maximum rated depth, see Table
 1062 1) were launched (~7% of the total) in the few campaigns in which the acquisition system showed significant

Deleted: an

Deleted: relative

Deleted: s at each meter of depth

Deleted: (a)

Deleted: b

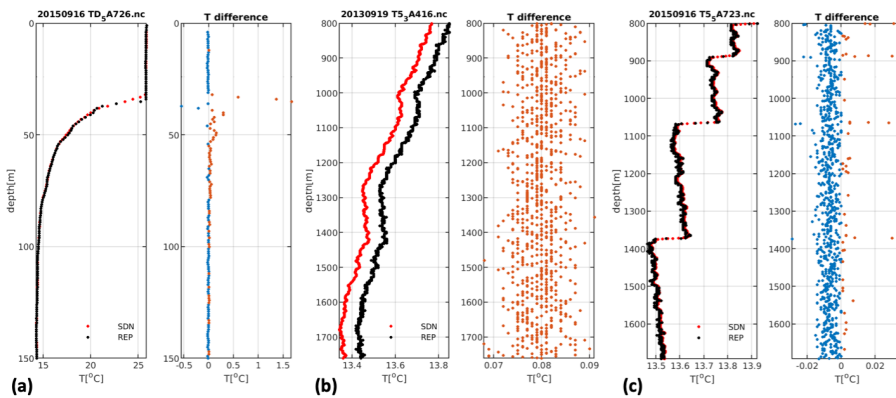
Deleted: s

Deleted: frequent step-like shape of the profile, due to double diffusion processes

Deleted: (Meccia et al. 2016; Durante et al., 2021),

Deleted: s

1079 [negative anomalies and this influenced both BIAS and RMSD profiles below 900 m depth. The frequent step-](#)
 1080 [like shape of deep profiles \(Figure 12c\), due to double diffusion processes \(Meccia et al. 2016; Durante et al.](#)
 1081 [2021\), causes instead positive spikes in the difference profiles.](#)
 1082 In the SDN dataset, the interpolation of raw profiles at each meter depth has been combined with the
 1083 application of a Gaussian filter to reduce possible noise (Manzella et al., 2003 and 2007). Consequently, a
 1084 general smoothing of T profiles is observed, which is appreciable to remove/reduce unrealistic high frequency
 1085 oscillations, if needed, but it also affects the values of the whole profile. The main effect is that the shape of
 1086 thermal structures is smoothed out, more or less evidently depending on the recorded T gradient,



1087
 1088 **Figure 12** Example of a reprocessed (REP) profile and the corresponding SeaDataNet (SDN) one **on the left and**
 1089 **their difference on the right: (a) zoom in the surface layer 0-150 m; (b and c) zoom in the bottom layer below 800**
 1090 **m.**

1091 **6. Summary and Conclusions**

1092 This work presents the reprocessing of XBT profiles in the Ligurian and Tyrrhenian Seas over the time period
 1093 1999-2019. The added value of this analysis is the availability of the original raw data and all the metadata
 1094 from the operational manual notes. This allowed us to create the most complete dataset possible with metadata
 1095 accompanying each individual T profile. The surface measurements have been added with quality indication
 1096 and a correction from calibration has been applied, when available, to T values (generally in the range 0.01-
 1097 0.02 °C), representing the best estimate of the thermal offset due to the operating XBT system characteristics.
 1098 A new automatic QC procedure and a new vertical interpolation (Barker and McDougall, 2020) have been
 1099 implemented without the application of any filter that: on one side, removes unrealistic high frequency
 1100 oscillations, and on the other, it smooths out the thermal structure of the T profiles with main impact on the
 1101 surface layer during stratified conditions. The adoption of a Gaussian filter [in SDN data \(Manzella et al., 2003;](#)
 1102 [2007\)](#) was justified by the purpose of assimilating XBT profiles in the Mediterranean Forecasting System that
 1103 in the early 2000s was characterized by a much lower resolution compared to the present numerical model
 1104 capabilities. [Cheng et al. \(2014\) XBT bias correction scheme for both temperature and depth records has also](#)

Deleted: ¶ ... [2]

Deleted: whole

Deleted: profiles on the left and relative difference profile on the right

Deleted:) zoom in the surface layer 0-150 m (

Deleted: 500-

Deleted:

Deleted: from

Deleted: (

Deleted: .

1119 [been applied to the calibrated profiles, in agreement with the recent literature, to facilitate the REP dataset](#)
1120 [integration with other data types for climate studies.](#) The REP dataset gives researchers the most complete
1121 information for its re-use for different applications (assimilation in ocean and climate models, process and
1122 climate studies). It can also be used to test new QC algorithms or the order on which to apply them to further
1123 improve the data quality.

1124 The adoption of FAIR data management principles through the use of SeaDataNet standards and the
1125 dissemination strategy based on the ERDDAP server implementation are additional values of this effort,
1126 allowing its machine to machine access.

1127 XBTs are a 60-year-old technology. Though the quality of their measurements might not fit the purpose of all
1128 applications and they leave debris in the ocean, “XBTs provide the simplest and most cost-efficient solution
1129 for frequently obtaining temperature profiles along fixed transects of the upper ocean” (Parks et al., 2022)
1130 using ships of opportunity. Moreover, the XBT measurements along the MX04 track were for some periods
1131 among the few measurements recorded in the Tyrrhenian and Ligurian Seas. Despite the limitations of the
1132 XBT characteristics, they constituted the simplest way to verify the physical state of the upper layer of those
1133 basins. It is therefore very important to provide those profiles with the best quality and usability indications.
1134 For this reason, the MX04 line has been re-established [on a seasonal base](#) in the framework of the MACMAP
1135 project after a two-year break [for climate monitoring.](#)

1136 In recent years, the use of XBTs has also been criticized because all probe components fall to the seabed.
1137 Given the current MACMAP sampling strategy with 37 launches in [fixed and determined positions along the](#)
1138 [MX04 line](#), the quantity of material abandoned at sea for each campaign can be easily estimated (about 22 kg
1139 of ZAMAK, just over 2 kg of plastic and about 11 kg of copper wire). [It would be preferably that](#) the XBT
1140 probes were made [of alternative materials \(e.g. iron "nose" and biodegradable plastic components\)](#), [however,](#)
1141 [in our cost-benefit analysis,](#) the environmental impact due to the [REP dataset is balanced](#) by the scientific
1142 results. [Finally,](#) the deployment of the XBT probes described here did not contribute to additional emissions
1143 of CO2 and other atmospheric pollutants, because only [ships of opportunity](#) were used and in the case of
1144 research vessels, the launch of the XBT probes was ancillary to the primary [purpose of the scientific cruise.](#)

1145 7. Data Availability and FAIRness

1146 The management of the REP dataset has been conceived since the beginning to be compliant with the FAIR
1147 [data management principles](#) (Wilkinson et al., 2016) and the open science paradigm. The REP dataset
1148 (Reseghetti et al., 2024; https://doi.org/10.13127/rep_xbt_1999_2019_2) is available and accessible through
1149 INGV (Bologna) ERDDAP server (<http://oceano.bo.ingv.it/erddap/index.html>), which allows machine to
1150 machine data access and gives to the users the possibility to select among several download formats. The raw
1151 data with [calibration information, bias correction](#) and the interpolated data [at standard depths](#) after data QC are
1152 released [with complete metadata description](#) together with all the processing information in order to facilitate
1153 data reuse. The format and the standards adopted for the dissemination of the REP dataset are described in

Deleted: on a seasonal base

Deleted: a

Deleted: f

Deleted: with

Deleted: other

Deleted:), it would certainly be better

Deleted: .

Deleted: H

Deleted: in a

Deleted: balance

Deleted: collection of profiles included in this

Deleted: exceeded

Moved down [2]: The use of XBTs allows the planning of monitoring surveys with only 24-36 hours advance notice, along a specific path including coastal areas, using merchant vessels.

Deleted: The MX04 transect has provided a series of tomographic-like "thermal images" along essentially the same path since September 1999, monitoring the area over the years and the occurrence of transient events and their evolution to be analyzed. The use of XBTs allows the planning of monitoring surveys with only 24-36 hours advance notice, along a specific path including coastal areas, using merchant vessels.

Moved (insertion) [2]

Deleted: commercial vessels

Deleted: activities

Deleted: for which the campaign was planned

Deleted: (Findable, Interoperable, Accessible, Reusable)

Deleted: 3

Field Code Changed

Deleted: h

Formatted: Default Paragraph Font, Font color: Custom Color(17,85,204)

Deleted: https://doi.org/10.13127/rep_xbt_1999_2019

Deleted: complete metadata description

1186 detail in Appendix C. The ODV collection of the REP interpolated dataset, used for the visual check, is also
1187 available on request.

1188

1189 **Author contribution**

1190 SS conceptualized the work, FR curated the original data (collecting a significant portion of it), CF developed
1191 the QC software, under the methodology supervision of SS, FR and LC. GR prepared the correction from the
1192 calibration of DAQs. CF manages and curates the reprocessed dataset. SS, FR and CF prepared the manuscript
1193 with contributions from GR and LC.

1194

1195 **Competing interests**

1196 S. Simoncelli is a member of the editorial board of the journal. Co-authors declare that they have no conflict
1197 of interest.

1198

1199 **Acknowledgements**

1200 We thank all people/institutions/companies involved in the data taking:

- 1201 • The Italian shipping company GNV, a very special partner that has allowed the monitoring activity
1202 since September 1999: in particular Marco Fasciolo, Dr. Mattia Canevari, the captains, the officers
1203 and all the crews for their precious collaboration;
- 1204 • Persons involved in data collection on the MX04 line, namely M. Borghini, F. Dell'Amico, C.Galli,
1205 E. Lazzone (CNR-ISMAR), M. Morgigni and A. Baldi (ENEA-STE);
- 1206 • CNR-ISMAR-Lerici for the very long collaboration that has allowed the acquisition of numerous XBT
1207 profiles from research vessels, in particular the crew and technicians of the RV Urania;
- 1208 • The international shipping companies Hapag Lloyd, CMA CGM and Arkas, their managers and crews
1209 for their valuable collaboration;
- 1210 • Responsible officers ashore and on board, crews and technicians of ships belonging to IIM, in
1211 particular CF Maurizio Demarte and Dr. Luca Repetti.
- 1212 • Australian government agency CSIRO for its kind cooperation by sharing their instrumentation in the
1213 2007-2011 data collection on container ships, notably Dr. Ann Thresher, Dr. Lisa Krummel and
1214 Rebecca Cowley;
- 1215 • The Federal Research Laboratory NOAA-AOML of Miami (FL), in particular Dr. Gustavo Goni and
1216 Dr. Francis Bringas, for the supply of the XBT probes used during some MX04 campaigns and for the
1217 support in carrying out the operational activities;
- 1218 • Stefano Latorre (INFN, Milan), key person in the development and implementation of the testers and
1219 their periodic calibration;
- 1220 • One of the authors (FR) for having supplied his own instrumentation and XBT probes for carrying out
1221 oceanographic campaigns since 2008.

Deleted: (Grandi Navi Veloci)

Deleted: Dr.

1224 A very special thanks to Giuseppe M. Manzella, who created the SOOP program in the Mediterranean Sea and
1225 coordinated it until 2013 and was among the pioneers in the development of marine data infrastructures. He
1226 supported this paper, providing useful comments.
1227 We acknowledge Marjahn Finlayson for reviewing the English, and Mario Locati (head of the INGV data
1228 management office) for his continuous support. This work has been developed in the framework of the
1229 MACMAP project, funded by Istituto Nazionale di Geofisica e Vulcanologia (Environment Department), and
1230 coordinated by Antonio Guarnieri that we thank.
1231

Formatted: Border: Top: (No border), Bottom: (No border),
Left: (No border), Right: (No border), Between : (No border)

Deleted: .

Deleted:

1234 **Appendix A**

1235 **Characteristics of test canisters**

1236 While in the laboratory, it is easy to have steady and controlled environmental conditions for measurements,
 1237 in the field, this is only an aspiration of the operators. Furthermore, repeated operation in conditions of high
 1238 temperature, humidity and salinity certainly does not facilitate the proper functioning of the electronic
 1239 instrumentation. The DAQ in an XBT system should read the nominal value of a resistance (within the
 1240 uncertainties of the measurements), showing no changes in its reading over time. The use of a tester with high
 1241 quality resistors is the preferred method to verify this. Between 2007 and 2010, two testers were built using
 1242 very high precision resistors (model KOA-Speer RN73r1jtt1002b10) combined in such a way as to achieve
 1243 corresponding T values similar to the extreme ones measured in the marine regions under investigation. The
 1244 resistance values of both testers were checked each year with a Wavetek Datron 1281 8.5 digits multi-meter
 1245 in a laboratory of the INFN (Italian National Institute of Nuclear Physics) in Milan (room temperature always
 1246 in the range 20-24 °C during measurements). The reading remained stable (within 0.1 Ohm) over the period
 1247 2008-2019 for the former and 2010-2015 for the latter.

Deleted: constant and under control

Deleted: the nominal value of a resistance

Deleted: because it is an essential component to get good quality XBT measurements

1248 **Table A1 - The resistance values measured in the control tests with the corresponding temperature values**
 1249 **calculated by a Hoge_2 equation for the two testers used in the XBT data acquisition campaigns since 2010.**

Model	Resistance 1 (Ohm)	Temperature 1 (°C)	Resistance 2 (Ohm)	Temperature 2 (°C)
Test canister 1	4631.0 ± 0.1	26.758 ± 0.001	8960.1 ± 0.1	12.197 ± 0.001
Test canister 2	4397.2 ± 0.1	27.956 ± 0.001	8725.3 ± 0.1	12.759 ± 0.001

1250
 1251 The resistance R values shown in Table A1 are then converted to T by applying the Hoge_2 R to T equation
 1252 (Sippican, 1991 and 2010; Hoge, 1988; Chen, 2009; Liu et al., 2018)

$$T = \frac{1}{A + B(\ln R) + C(\ln R)^2 + D(\ln R)^3} - 273.15^\circ\text{C}$$

1254 with the following coefficients: $A = 1.2901230 \cdot 10^{-3}$, $B = 2.3322529 \cdot 10^{-4}$, $C = 4.5791293 \cdot 10^{-7}$, $D =$
 1255 $7.1625593 \cdot 10^{-8}$

Formatted: Justified

Deleted: ¶

Deleted: e-3¶

1256 To our knowledge, this equation and the coefficients remained unchanged since the 1990s for all the DAQs,
 1257 namely Sippican MK12, MK21 ISA, MK21 USB, MK21 Ethernet, Turo Devil, Turo Quoll. Sippican used the
 1258 Steinhart-Hart relation for its MK9 model (IOC, 1992) while tabulated R to T values were used for MK-2A
 1259 and similar recorders (Sippican, 1968; Plessey, 1975).

Deleted: e-7¶

Deleted: e-4¶

Deleted: e-8

Deleted: associated

Deleted: used.

1260
 1261

1275 **Appendix B**

1276 **Table B1 - Summary of ships, instrumentation and operating conditions during the collection of the XBT profiles**
 1277 **in the REP dataset.**

Deleted: ome details
 Deleted: included
 Deleted: for all the ships participating the measurements

Ship Name	Call Sign/ IMO No.	Number of Campaigns	Years of Activity	DAQ used	Height launch (m)	Range of ship speed (knöts)
Excelsior	IBEX 9184419	20 1 7	1999-2000 2012 2017-2018	MK12 MK21 USB MK21 Ethernet	10±0.5	20-24
Excellent	IBBE 9143441	1 5	2004 2012-2014	MK21 ISA MK21 USB	10±0.5	19-24
Splendid	IBAS 9015747	1	2011	MK21 USB	10±0.5	20-22
La Superba	ICGK 9214276	14 1 23 1 3	2004-2006 2010 2010-2016 2011 2016-2017	MK21 ISA TURO QUOLL MK21 USB MK12 MK21 Ethernet	11±0.5	21-28
La Suprema	IBIL 9214288	2 6 6	2004 2011-2016 2016-2019	MK21 ISA MK21 USB MK21 Ethernet	11±0.5	21-28
Wellington Express	DFCX2 9224051	5	2007-2008	TURO DEVIL	25±1.0	14-20
Canberra Express	DFCW2 9224049	1	2008	TURO DEVIL	25±1.0	14-20
Stadt Weimar	DCHO 9320051	8	2009-2010	TURO DEVIL	27±1.0	14-20
CMA CGM Charcot	A8HE4 9232773	5	2009-2011	TURO DEVIL	25±1.0	14-20
Daniel A	TCLA 9238064	2	2014	MK21 USB	8±0.5	14-17
Ammiraglio Magnaghi	IGMA 8642751	3 1 2	2008-2013 2011 2019	MK12 MK21 USB TURO QUOLL	(3 – 6) ±0.5	1-10
Aretusa	IABA	1 2	2006 2017-2018	MK12 MK21 USB	(4 – 5) ±0.5	1-10
Galatea	IABC	1	2013	MK12	(4 – 5) ±0.5	1-10
Urania	IOSU 9013220	12 13	2000-2012 2005-2014	MK12 MK21 USB	(3 – 12) ±0.5	0-11
Minerva 1	IZVM 9262077	1 1	2015 2016	MK21 USB MK21 Ethernet	(3 – 8) ±0.5	0-11
Ibis	--	1	2019	MK21 Ethernet	3 ±0.5	0-10

1278

1279

1283 **Appendix C**

1284 **Format and standards**

1285 The data format adopted to archive the REP dataset is the NetCDF (Network Common Data Form). It is self-
1286 describing since it includes the metadata that describe both data and data structures. The NetCDF
1287 implementation is based on the community-supported Climate and Forecasts (CF) specification (CF1.6 profile
1288 for profile data) and it adopts the SeaDataNet vocabularies ([https://www.seadatanet.org/Standards/Common-](https://www.seadatanet.org/Standards/Common-Vocabularies)
1289 [Vocabularies](https://www.seadatanet.org/Standards/Common-Vocabularies)). The reference SDN parameter codes (P01 terms,
1290 https://vocab.seadatanet.org/v_bodc_vocab_v2/search.asp?lib=P01) and the associated standard units (P06
1291 terms https://vocab.seadatanet.org/v_bodc_vocab_v2/search.asp?lib=P06) are used in order to ensure the
1292 proper interpretation of values by both humans and machines and to allow data interoperability in terms of
1293 manipulation, distribution and long-term reuse.

1294 Each XBT NetCDF file contains:

- 1295 • **dimensions** that provide information on the size of the variables (a.k.a. “parameters”);
- 1296 • **coordinate variables** that orient the data in time and space;
- 1297 • **geophysical variables** that contain the actual measurements;
- 1298 • **ancillary variables** that contain the quality information (QFs) values;
- 1299 • **additional variables** that include some of the variables being part of SDN extensions to CF;
- 1300 • **global metadata fields** that refer to the whole file, not just to one variable (a.k.a. “global attributes”).

1301 **C.1 Dimensions**

1302 The pattern followed by SDN for “profiles” data type is to have an ‘INSTANCE’ unlimited dimension plus a
1303 maximum number of z coordinate levels (*MAXZ*). We included also string size dimension *STRING* for text
1304 arrays and added test size dimensions referring respectively to test QFs on temperature (*TST_T*) and depth
1305 (*TST_D*) values and the maximum number of z coordinate levels for the data re-sampled at a 1 m interval, after
1306 the QC is applied (*MAX_INT*).

1307 **C.2 Coordinate variables**

1308 NetCDF coordinates are a special subset of variables which orient the data in time and space. They are:

- 1309 • LONGITUDE for x;
- 1310 • LATITUDE for y;
- 1311 • TIME for t;
- 1312 • DEPTH for z.

1313 **C.3 Geophysical variables**

1314 Each file contains:

- 1315 • depth: depth at original vertical resolution;

Deleted: n

Deleted: point

Deleted: (SDN)

Deleted: Quality Flags,

Deleted: Quality Check (

Deleted:)

- 1322 ● TEMPET01: Calibrated sea water temperature at original vertical resolution;
- 1323 ● DEPTH_COR: Original vertical resolution depth corrected by applying Cheng et al. (2014);
- 1324 ● TEMPET01_COR: Calibrated and corrected sea water temperature as resulting by applying Cheng et
1325 al. (2014);
- 1326 ● DEPTH_INT: depth interpolated on standard depth levels using Barker & McDougall (2020) method;
- 1327 ● TEMPET01_INT: TEMPET01 interpolated on standard depth levels using Barker & McDougall
1328 (2020) method;
- 1329 ● DEPTH_COR_INT: DEPTH_COR interpolated on standard depth levels using Barker & McDougall
1330 (2020) method;
- 1331 ● TEMPET01_COR_INT: TEMPET01 COR interpolated on standard depth levels (each meter depth)
1332 using Barker & McDougall (2020) method;

Formatted: Font: 11 pt

Deleted: <#>full resolution raw Temperature (T) data corrected via calibration based on tester check (when available) and,

Deleted: <#>interpolated data at each meter depth

Deleted: <#> as well

1333 Calibration values are provided in a separate variable CALIB, so that experts can trace back the raw
1334 (uncalibrated) profile if needed.

1335 For each coordinate and geophysical variable four mandatory parameter attributes are included, as defined in
1336 Lowry et al. (2019):

- 1337 1. *sdn_parameter_urn*: this is the URN (Uniform Resource Name) for the parameter description taken
1338 from the P01 vocabulary;
- 1339 2. *sdn_parameter_name*: this is the plain language label (Entryterm) for the parameter taken from the
1340 P01 vocabulary at the time of the data creation;
- 1341 3. *sdn_uom_urn*: this is the URN for the parameter units of measurement taken from the P06 vocabulary;
- 1342 4. *sdn_uom_name*: this is the plain language label (Entryterm) for the parameter taken from the P06
1343 vocabulary at the time of data file creation.

1344 Moreover, since some of the coordinate variable names could be ambiguous, particularly for the z-coordinate,
1345 we adopt the standard_name (P07 vocabulary,
1346 https://vocab.seadatanet.org/v_bodc_vocab_v2/search.asp?lib=P07), not mandatory in CF but widely used,
1347 which significantly enhances interoperability.

1348 C.4 Ancillary variables

1349 In order to report data quality information on a point by point basis, every measurement is tagged with a single-
1350 byte encoded label referred to as a ‘flag’. The flag variables are mandatory for all coordinate and geophysical
1351 variables to which they relate through ‘ancillary_variables’ in the parent variable set to the name of ancillary
1352 variable attribute (Lowry et al., 2019). The flags are encoded using the SDN L20 vocabulary
1353 (https://vocab.seadatanet.org/v_bodc_vocab_v2/search.asp?lib=L20) and each ancillary variable carries
1354 attributes ‘flag_values’ and ‘flag_meanings’, which provide a list of possible values and their meanings.

1355 For coordinate variables, the ancillary variables are the following:

- 1356 ● TIME_SEADATANET_QC: it is the ancillary variable referring to TIME parent variable;

1362 • POSITION_SEADATANET_QC: Longitude and latitude flag variables are combined into a single
1363 flag for 'position', following OceanSITES (2020) practice.

1364 For depth coordinate, the ancillary variables are:

- 1365 • DEPTH_TEST_QC: it contains flags coming from the application of depth check test;
- 1366 • DEPTH_FLAGS_QC: it contains flags associated with each original depth value and summarizes the
1367 results of the performed depth test check mapped on SDN L20 vocabulary;
- 1368 • DEPTH_COR_FLAGS_QC: it contains flags associated with each corrected (Cheng et al., 2014;
1369 CH14) depth value;
- 1370 • DEPTH_INT_SEADATANET_QC: it contains flags associated with the interpolated profile;
- 1371 • DEPTH_COR_INT_SEADATANET_QC: it contains flags associated with the corrected (CH14)
1372 interpolated profile.

1373 For temperature geophysical variable, the ancillary variables, similarly to depth coordinate, are the following:

- 1374 • TEMPET01_TEST_QC: it contains exit values coming from the application of independent
1375 temperature check tests;
- 1376 • TEMPET01_FLAGS_QC: it contains the QFs associated with each calibrated temperature value and
1377 summarizes the results of the performed independent temperature test checks mapped on SDN L20
1378 vocabulary;
- 1379 • TEMPET01_COR_FLAGS_QC: it contains the QFs associated with each calibrated and corrected
1380 (CH14) temperature value;
- 1381 • TEMPET01_INT_SEADATANET_QC: it contains QFs associated with the temperature interpolated
1382 profile;
- 1383 • TEMPET01_COR_INT_SEADATANET_QC: it contains QFs associated with the corrected (CH14)
1384 temperature interpolated profile

1386 C.5 Additional variables

1387 In addition to attributes, some variables from the SDN extension have been adopted:

- 1388 1. SDN_CRUISE: an array containing the name of project which funded the cruise;
- 1389 2. SDN_EDMO_CODE: an integer array containing keys identifying the organization in the European
1390 Directory of Marine Organizations (EDMO, <https://www.seadatanet.org/Metadata/EDMO-Organisations>)
1391
- 1392 3. SDN_BOT_DEPTH: a floating point array holding bathymetric water depth in meters where the
1393 sample was collected or measurement was made. We considered the local bottom depth extracted from
1394 the GEBCO Compilation Group (2021).

1395 In order to preserve and keep track of metadata associated with each profile in the dissemination through
1396 ERDDAP, other variables have been adopted:

- 1397 4. cruise_id: an array containing the name of the project which funded the cruise plus the year and the
1398 month of the cruise;

Deleted: re are three different

Deleted: .

Deleted: flags

Deleted: flags

Deleted: original

Deleted: flags

Deleted: .

Deleted: Moreover, i

1407 5. profile_id: an array referring to the sequence of the profile during the corresponding cruise.

1408 C.6 Global metadata fields

1409 The global attribute section of the NetCDF file describes its content overall. All attributes should be human-
1410 readable and contain meaningful information for data discovery and re-use. Most importantly, all available
1411 discovery metadata to the SDN mandatory attributes have been introduced following recommendations of the
1412 XBT community. Moreover, several studies (Cheng et al., 2014; 2016; 2018; Goni et al., 2019) highlighted
1413 the dependency of the biases on probe type, time (due to variations in the manufacturing process) and changes
1414 in the recording systems (Tan et al., 2021). For these reasons, the following information has been inserted in
1415 the XBT metadata description: probe type with serial number, manufacturer, manufacturing date, FRE
1416 coefficients used to calculate the depth, launch height, DAQ model and recorder version (Cheng et al., 2016).

1417 Ship speed, wind speed, and probe mass (available since 2018) have been added to this metadata section, when
1418 available.

1419 The depth (depth_uncertainty) and temperature (TEMPET01_uncertainty) uncertainties, being equal to each
1420 profile within the REP dataset, have been included as global attributes.

1421 The above mentioned information has been kept and made available through the ERDDAP by an url_metadata
1422 variable associated to each profile. The following python code can be used to retrieve the specific information
1423 for each profile:

```
1424 from erddapy import ERDDAP  
1425 import urllib.request  
1426 import json  
1427 import pandas as pd  
1428 import numpy as np  
1429 e=ERDDAP(  
1430     server="http://oceano.bo.ingv.it/erddap",  
1431     protocol="tabledap"  
1432 )  
1433 e.dataset_id='REP XBT 1999 2019'  
1434 # Select parameters of interest  
1435 e.variables = ['url_metadata']  
1436 df=e.to_pandas()  
1437 url=(df['url_metadata'])  
1438 # Select profile of interest  
1439 profile='MFSPP 990920 011'  
1440 index=[idx for idx, s in enumerate(url) if profile in s][0]  
1441 new_url=url[index].replace('htmlTable','json')  
1442 response=urllib.request.urlopen(new_url)  
1443 string=response.read()  
1444 json_obj = json.loads(string)  
1445 element=(json_obj['table'].get('columnNames'))  
1446 element_values=(json_obj['table'].get('rows')[0])  
1447 infor=pd.DataFrame({'Elements':element,'Values':element_values})  
1448 #Select information of interest  
1449 lst_gdpt=(infor.Values[infor.Elements=='LAST GOOD DEPTH ACCORDING TO OPERATOR'])  
1450 print('for profile: '+profile+' last good depth according to operator is:  
1451  '+str(lst_gdpt.values[0])+'m')  
1452
```

1453

1454

Deleted: . W

Deleted: , mass of the XBT probe, wind speed and ship speed are other useful information included in this metadata section

Deleted: the entire dataset

Deleted: , which contains details specific to each profile

Formatted: English (US)

1460 **References**

- 1461 Anderson, E.A.: Expendable bathythermograph (XBT) accuracy studies, Tech. Rep. 550, Naval Ocean System
1462 Center, California, 201 pp, June 1980. <https://doi.org/10.5962/bhl.title.47513>, 1980.
- 1463 Bailey, R., Gronell A., Phillips H., Tanner E. and Meyers G.: Quality Control Cookbook for XBT Data. CSIRO
1464 Report 221, 84 pp, 1994. <http://hdl.handle.net/102.100/237126?index=1>
- 1465 Barker, P.M., and McDougall, T.J.: Two Interpolation Methods Using Multiply-Rotated Piecewise Cubic
1466 Hermite Interpolating Polynomials. *J. Atmos. Oceanic Technol.*, 37(4), 605–619.
1467 <https://doi.org/10.1175/JTECH-D-19-0211.1>, 2020.
- 1468 Bordone, A., Pennechi F., Raiteri G., Repetti L., Reseghetti F.: XBT, ARGO Float and Ship-Based CTD
1469 Profiles Intercompared under Strict Space-Time Conditions in the Mediterranean Sea: Assessment of
1470 Metrological Comparability. *Journal of Marine Science and Engineering*, 8(5):313.
1471 <https://doi.org/10.3390/jmse8050313>, 2020.
- 1472 Bringas, F., and Goni, G.: Early dynamics of Deep Blue XBT probes, *J. Atmos. Oceanic Technol.*, 32(12),
1473 2253–2263. <https://doi.org/10.1175/JTECH-D-15-0048.1>, 2015.
- 1474 Chen, C.: Evaluation of resistance–temperature calibration equations for NTC thermistors. *Measurement*, 42,
1475 1103–1111, doi:10.1016/j.measurement.2009.04.004.
- 1476 Cheng, L., Abraham, J., Trenberth, K.E. et al. Another Record: Ocean Warming Continues through 2021
1477 despite La Niña Conditions. *Adv. Atmos. Sci.* 39, 373–385 (2022). [https://doi.org/10.1007/s00376-022-1461-](https://doi.org/10.1007/s00376-022-1461-3)
1478 [3](https://doi.org/10.1007/s00376-022-1461-3)
- 1479 Cheng, L., Abraham, J., Trenberth, K.E. et al. Upper Ocean Temperatures Hit Record High in 2020. *Adv.*
1480 *Atmos. Sci.* 38, 523–530 (2021). <https://doi.org/10.1007/s00376-021-0447-x>
- 1481 Cheng, L., Abraham, J., Zhu, J. et al. Record-Setting Ocean Warmth Continued in 2019. *Adv. Atmos. Sci.* 37,
1482 137–142 (2020). <https://doi.org/10.1007/s00376-020-9283-7>
- 1483 Cheng, L., and Coauthors: How well can we correct systematic errors in historical XBT data? *J. Atmos.*
1484 *Oceanic Technol.*, 35, 1103–1125, doi:10.1175/jtech-d-17-0122.1, 2018.
- 1485 Cheng, L., et al., Improved estimates of ocean heat content from 1960 to 2015. *Sci. Adv.* 3,e1601545 (2017).
1486 DOI:10.1126/sciadv.1601545
- 1487 Cheng, L., and Coauthors: XBT science: assessment of instrumental biases and errors. *Bull. Amer. Meteor.*
1488 *Soc.* 97, 923–934, doi:10.1175/Bams-D-15-00031.1, 2016.
- 1489 Cheng, L., J. Zhu, R. Cowley, T. Boyer, and S. Wijffels: Time, probe type, and temperature variable bias
1490 corrections to historical expendable bathythermograph observations. *J. Atmos. Oceanic Technol.*, 31, 1793–
1491 1825, doi:10.1175/Jtech-D-13-00197.1, 2014.
- 1492 Cook, S. and Sy A.: Best guide and principles manual for the Ships Of Opportunity Program (SOOP) and
1493 eXpendable BathyThermograph (XBT) operations, Geneva, Switzerland, WMO & IOC, 26pp. DOI:
1494 <https://doi.org/10.25607/OBP-1483>.
- 1495 Cowley R., Killick R.E., Boyer T., Gouretski V., Reseghetti F., Kizu S., Palmer M.D., Cheng L., Storto A., Le
1496 Menn M., Simoncelli S., Macdonald A.M. and Domingues C.M.: International Quality-Controlled Ocean
1497 Database (IQuOD) v0.1: The Temperature Uncertainty Specification. *Front. Mar. Sci.* 8:689695. doi:
1498 10.3389/fmars.2021.689695, 2021.

- 1499 Cowley, R., and Krummel, L.: Australian XBT Quality Control Cookbook Version 2.0. Report EP2022-1825
1500 CSIRO, Australia, pp. 1-89 <https://doi.org/10.25919/3tm5-zn80>, 2022.
- 1501 Durante S, Oliveri P, Nair R and Sparnocchia S (2021) Mixing in the Tyrrhenian Interior Due to Thermohaline
1502 Staircases. *Front. Mar. Sci.* 8:672437. doi: 10.3389/fmars.2021.672437
- 1503 Flierl, G. R., and A. R. Robinson, 1977: XBT Measurements of Thermal Gradients in the MODE Eddy. *J.*
1504 *Phys. Oceanogr.*, 7, 300–302, [https://doi.org/10.1175/1520-0485\(1977\)007<0300:XMOTGI>2.0.CO;2](https://doi.org/10.1175/1520-0485(1977)007<0300:XMOTGI>2.0.CO;2).
- 1505 Fusco, G., Manzella, G. M. R., Cruzado, A., Gacic, M., Gasparini, G. P., Kovacevic, V., Millot, C., Tziavos,
1506 C., Velasquez, Z., Walne, A., Zervakis, V., and Zodiatis, G.: Variability of mesoscale features in the
1507 Mediterranean Sea from XBT data analysis, *Ann. Geophys.*, 21, 21–32, [http://www.ann-](http://www.ann-geophys.net/21/21/2003/)
1508 [geophys.net/21/21/2003/](http://www.ann-geophys.net/21/21/2003/), 2003.
- 1509 GEBCO Compilation Group: GEBCO 2021 Grid. doi:10.5285/c6612cbe-50b3-0cff-e053-6c86abc09f8f,
1510 2021.
- 1511 Goni, G., and Coauthors: More than 50 years of successful continuous temperature section measurements by
1512 the global expendable bathythermograph network, its integrability, societal benefits, and future. *Front. Mar.*
1513 *Sci.*, 6:452, doi:10.3389/fmars.2019.00452, 2019.
- 1514 Haddad, S., R. E. Killick, M. D. Palmer, M. J. Webb, R. Prudden, F. Capponi, and S. V. Adams, 2022:
1515 Improved Infilling of Missing Metadata from Expendable Bathythermographs (XBTs) Using Multiple
1516 Machine Learning Methods. *J. Atmos. Oceanic Technol.*, 39, 1367–1385, [https://doi.org/10.1175/JTECH-D-](https://doi.org/10.1175/JTECH-D-21-0117.1)
1517 [21-0117.1](https://doi.org/10.1175/JTECH-D-21-0117.1).
- 1518 Hanawa, K., P. Rual, R. Bailey, A. Sy, and M. Szabados: A new depth-time equation for Sippican or TSK T-
1519 7, T-6 and T-4 expendable bathythermographs (XBT). *Deep-Sea Res. I*, 42, 1423–1451, doi:10.1016/0967-
1520 0637(95)97154-Z, 1995.
- 1521 Hoge, H.: Useful procedure in least squares, and tests of some equations for thermistors. *Rev. Sci. Instrum.*,
1522 59, 975-979, doi:10.1063/1.1139762, 1988.
- 1523 [Intergovernmental Oceanographic Commission \(1975\). Manuals and guides, 4. Guide to oceanographic and](#)
1524 [marine meteorological instruments and observing practices. pp. 1-78. ISBN 92-3-101325-4](#)
- 1525 [Intergovernmental Oceanographic Commission \(1992\). Ad hoc meeting of the IGOSS Task Team on quality](#)
1526 [control for automated systems. Marion, Massachusetts, USA, 3–6 June 1991. Intergovernmental](#)
1527 [Oceanographic Commission IOC/INF-888, pp. 1-144.](#)
- 1528 [Intergovernmental Oceanographic Commission \(1997\). First Session of the Joint IOC-WMO IGOSS Ship-of-](#)
1529 [Opportunity Programme Implementation Panel: Annex VI, Cape Town, South Africa, 16–18 April 1997, pp.](#)
1530 [1-46.](#)
- 1531 Intergovernmental Oceanographic Commission (2013) Ocean Data Standards Volume 3. Recommendation for
1532 a Quality Flag Scheme for the Exchange of Oceanographic and Marine Meteorological Data. Paris, France,
1533 UNESCO-IOC, 5pp. & Annexes. (Intergovernmental Oceanographic Commission Manuals and Guides,
1534 Volume 54 (3). (IOC/2013/MG/54-3) <http://dx.doi.org/10.25607/OBP-6>.
- 1535 Intergovernmental Oceanographic Commission (2019) Ocean Data Standards Volume 4: Technology for
1536 SeaDataNet Controlled Vocabularies for describing Marine and Oceanographic Datasets - A joint Proposal by
1537 SeaDataNet and ODIP projects. Oostend, Belgium, IODE/UNESCO, 31pp. (IOC Manuals and Guides, 54,
1538 Vol. 4. Version 1), (IOC/2019/MG/54 Vol.4). DOI: <http://dx.doi.org/10.25607/OBP-566>
- 1539 [Kizu, S., and K. Hanawa, 2002a: Start-up transient of XBT measurement. Deep-Sea Res. I, 49, 935–940,](#)
1540 [https://doi.org/10.1016/S0967-0637\(02\)00003-1](https://doi.org/10.1016/S0967-0637(02)00003-1).

- 1541 Leahy, T. P., F. P. Llopis, M. D. Palmer, and N. H. Robinson, 2018: Using Neural Networks to Correct
 1542 Historical Climate Observations. *J. Atmos. Oceanic Technol.*, 35, 2053–2059, <https://doi.org/10.1175/JTECH->
 1543 [D-18-0012.1](https://doi.org/10.1175/JTECH-D-18-0012.1).
- 1544 Li, Y., Church, J. A., McDougall, T.J., and Barker, P. M.: Sensitivity of observationally based estimates of
 1545 ocean heat content and thermal expansion to vertical interpolation schemes. *Geophysical Research Letters*, 49,
 1546 e2022GL101079. <https://doi.org/10.1029/2022GL101079>, 2022.
- 1547 [Little, A. D., Inc., 1965. Experimental evaluation of expendable bathythermographs. Dept. of the Navy Bureau](#)
 1548 [of Ships Rep. ASW Sonar Technology Report No. 4071165, Dept. of the Navy - Bureau of Ships Project SN](#)
 1549 [SF-101-03-21, Task 11353, November 1965, 51 pp.](#)
- 1550 [Little, A. D., Inc., 1966. Expendable bathythermograph \(XBT\) system evaluation for tactical sonar application.](#)
 1551 [ASW Sonar Technology Report No. 4150866, Dept. of the Navy - Naval Ship Systems Command, Project SN](#)
 1552 [SF-101-03-21, Task 11353, June 1966, 85 pp.](#)
- 1553 Liu, G., L. Guo, C. Liu, and Q. Wu: Evaluation of different calibration equations for NTC thermistor applied
 1554 to high-precision temperature measurement. *Measurement*, 120, 21-27,
 1555 doi:10.1016/j.measurement.2018.02.007, 2018.
- 1556 Lowry, R.; Fichaut, M. and Bregent S.: SeaDataNet NetCDF format definition. Version 1.21. SeaDataNet,
 1557 73pp. DOI: <http://dx.doi.org/10.25607/OBP-408>, 2019.
- 1558 [Magruder, P. M., Jr. "Some characteristics of temperature microstructure in the ocean". 1970, M.S. thesis,](#)
 1559 [Dept. of Oceanography, US Naval Postgraduate School, pp1-155.](#)
- 1560 Manzella, G. M. R., Scoccimarro, E., Pinardi, N., and Tonani, M.: "Improved near real time data management
 1561 procedures for the Mediterranean ocean Forecasting System – Voluntary Observing Ship Program", *Ann.*
 1562 *Geophys.*, 21, pp. 49–62. <https://doi.org/10.5194/angeo-21-49-2003>, 2003.
- 1563 Manzella, G. M. R., Reseghetti, F., Coppini, G., Borghini, M., Cruzado, A., Galli, C., Gertman, I., Gervais, T.,
 1564 Hayes, D., Millot, C., Murashkovsky, A., Özsoy, E., Tziavos, C., Velasquez, Z., and Zodiatis, G.: The
 1565 improvements of the ships of opportunity program in MFS-TEP, *Ocean Sci.*, 3, 245–258,
 1566 <https://doi.org/10.5194/os-3-245-2007>, 2007.
- 1567 Meccia, V. L., Simoncelli, S., & Sparnocchia, S. (2016). Decadal variability of the Turner Angle in the
 1568 Mediterranean Sea and its implications for double diffusion. *Deep Sea Research Part I: Oceanographic*
 1569 *Research Papers*, 114, 64–77. <https://doi.org/10.1016/J.DSR.2016.04.001>
- 1570 Meyssignac B., Boyer T., Zhao Z., et al.: Measuring Global Ocean Heat Content to Estimate the Earth Energy
 1571 Imbalance. *Front. Mar. Sci.* 6:432. <https://doi.org/10.3389/fmars.2019.00432>, 2019.
- 1572 Millot, C., Taupier-Letage, I. (2005a). Circulation in the Mediterranean Sea. In: Saliot, A. (eds) *The*
 1573 *Mediterranean Sea. Handbook of Environmental Chemistry*, vol 5K. Springer, Berlin, Heidelberg.
 1574 <https://doi.org/10.1007/b107143>
- 1575 Millot, C. and Taupier-Letage, I., 2005b: Additional evidence of LIW entrainment across the Algerian Basin
 1576 by mesoscale eddies and not by permanent westward-flowing vein, *Progress in Oceanography*, 231–250.
 1577 <https://doi.org/10.1016/j.pocean.2004.03.002>
- 1578 OceanSITES, 2020: OceanSITES Data Format Reference Manual NetCDF Conventions and Reference Tables.
 1579 Version 1.4 July 16, 2020. Geneva, Switzerland, OceanSITES, JCOMMOPS, 36pp. DOI:
 1580 <http://dx.doi.org/10.25607/OBP-421.2>

- 1581 Palmer, M. D., T. Boyer, R. Cowley, S. Kizu, F. Reseghetti, T. Suzuki, and A. Thresher, 2018: An Algorithm
 1582 for Classifying Unknown Expendable Bathythermograph (XBT) Instruments Based on Existing Metadata. *J.*
 1583 *Atmos. Oceanic Technol.*, 35, 429–440, <https://doi.org/10.1175/JTECH-D-17-0129.1>.
- 1584 Parks, J., Bringas, F., Cowley, R., Hanstein, C., Krummel, L., Sprintall, J., Cheng, L., Cirano, M., Cruz, S.,
 1585 Goes, M., Kizu, S. and Reseghetti, F., 2022: XBT operational best practices for quality assurance. *Front. Mar.*
 1586 *Sci.* 9:991760. doi: 10.3389/fmars.2022.991760
- 1587 Pinardi, N., Allen, I., Demirov, E., De Mey, P., Korres, G., Lascaratos, A., Le Traon, P.-Y., Maillard, C.,
 1588 Manzella, G., and Tziavos, C., 2003: The Mediterranean ocean forecasting system: first phase of
 1589 implementation (1998–2001), *Ann. Geophys.*, 21, 3–20, <https://doi.org/10.5194/angeo-21-3-2003>
- 1590 Pinardi, N., and Coppini, G., 2010: Preface" Operational oceanography in the Mediterranean Sea: the second
 1591 stage of development". *Ocean Science*, 6(1), 263-267, <https://doi.org/10.5194/os-6-263-2010>, 2010.
- 1592 Pinardi N, Stander J, Legler DM, O'Brien K, Boyer T, Cuff T, Bahurel P, Belbeoch M, Belov S, Brunner S,
 1593 Burger E, Carval T, Chang-Seng D, Charpentier E, Ciliberti S, Coppini G, Fischer A, Freeman E, Gallage C,
 1594 Garcia H, Gates L, Gong Z, Hermes J, Heslop E, Grimes S, Hill K, Horsburgh K, Iona A, Mancini S, Moodie
 1595 N, Ouellet M, Pissierssens P, Poli P, Proctor R, Smith N, Sun C, Swail V, Turton J and Xinyang Y (2019) The
 1596 Joint IOC (of UNESCO) and WMO Collaborative Effort for Met-Ocean Services. *Front. Mar. Sci.* 6:410. doi:
 1597 10.3389/fmars.2019.00410
- 1598 Plessey Company Limited, 1975: Plessey-Sippican expendable bathythermograph system, Tech. Rep.
 1599 MP0400, Issue 0401, January 1975, 51 pp.
- 1600 [Reid, W. L. Jr., 1964. Expendable Bathythermograph Evaluation. Oceanographic Instrumentation Center, US](#)
 1601 [Naval Oceanographic Office, December 1964, DTIC AD A045064, 78 pp.](#)
- 1602 R.F. Reiniger, C.K. Ross, 1968: A method of interpolation with application to oceanographic data, *Deep Sea*
 1603 *Research and Oceanographic Abstracts*, Volume 15, Issue 2, Pages 185-193, ISSN 0011-7471,
 1604 [https://doi.org/10.1016/0011-7471\(68\)90040-5](https://doi.org/10.1016/0011-7471(68)90040-5).
- 1605 Reseghetti, F., M. Borghini, and G. M. R. Manzella, 2007: Factors affecting the quality of XBT data—Results
 1606 of analyses on profiles from the Western Mediterranean Sea. *Ocean Science*, 3, 59–75,
 1607 <https://doi.org/10.5194/os-3-59-2007>
- 1608 Reseghetti, F., L. Cheng, M. Borghini, I. M. Yashayaev, G. Raiteri, and J. Zhu, 2018: Assessment of Quality
 1609 and Reliability of Measurements with XBT Sippican T5 and T5/20. *J. Atmos. Oceanic Technol.*, 35, 1935–
 1610 1960, <https://doi.org/10.1175/JTECH-D-18-0043.1>.
- 1611 [Reseghetti, F., Fratianni, C., & Simoncelli, S. \(2024\). Reprocessed XBT dataset in the Ligurian and Tyrrhenian](#)
 1612 [seas \(1999-2019\) \(Version 2\) \[dataset\]. Istituto Nazionale di Geofisica e Vulcanologia \(INGV\).](#)
 1613 https://doi.org/10.13127/REP_XBT_1999_2019.2
- 1614 Simoncelli, S., Schaap, D., Schlitzer, R., 2020a: Mediterranean Sea - Temperature and salinity Historical Data
 1615 Collection SeaDataCloud V2. <https://doi.org/10.12770/2a2aa0c5-4054-4a62-a18b-3835b304fe64>
- 1616 Simoncelli, S., Oliveri, P., Mattia, G., Myroshnychenko, V., 2020b: SeaDataCloud Temperature and Salinity
 1617 Historical Data Collection for the Mediterranean Sea (Version 2). Product Information Document (PIDoc).
 1618 <https://doi.org/10.13155/77059>
- 1619 S. Simoncelli, G. M.R. Manzella, A. Storto, A. Pisano, M. Lipizer, A. Barth, V. Myroshnychenko, T. Boyer,
 1620 C. Troupin, C. Coatanoan, A. Pitiitto, R. Schlitzer, Dick M.A. Schaap, S. Diggs, Chapter Four - A collaborative
 1621 framework among data producers, managers, and users, Editor(s): Giuseppe Manzella, Antonio Novellino,
 1622 *Ocean Science Data*, Elsevier, 2022, Pages 197-280, ISBN 9780128234273, [https://doi.org/10.1016/B978-0-](https://doi.org/10.1016/B978-0-12-823427-3.00001-3)
 1623 [12-823427-3.00001-3](https://doi.org/10.1016/B978-0-12-823427-3.00001-3)

Deleted: Reseghetti F., Fratianni C., Simoncelli S. (2023). Reprocessed of XBT dataset in the Ligurian and Tyrrhenian seas (1999-2019). Istituto Nazionale di Geofisica e Vulcanologia (INGV). https://doi.org/10.13127/rep_xbt_1999_2019

- 1629 Sippican Corp.: Instructions for installation, operation and maintenance of Sippican expendable
1630 bathythermograph system - M300, R-467B, 100 pp, 1968.
- 1631 Sippican: Instruction manual for the expendable bathythermograph system, R-603G - 1971, Sept. 1980. The
1632 Sippican Corporation Ocean Systems Division, 208 pp, 1980.
- 1633 [Sippican Ocean Systems, Inc.: XCTD Phase I Progress Report \(13 July 1983\). Contract N00014-82-C-0579.
1634 R-1259 - 1983. 66 pp. 1983.](#)
- 1635 Sippican, Inc.: Sippican MK12 oceanographic data acquisition system user's manual, Sippican, Inc., User's
1636 Manual R-2626/B P/N 306130-1, August 1991, 166 pp., 1991.
- 1637 Lockheed Martin Sippican (Sippican) Inc.: MK21 USB DAQ, surface ship, bathythermograph data acquisition
1638 system, installation operation and maintenance manual, P/N 308437, Rev. E, 172 pp, 2006.
- 1639 Lockheed Martin Sippican (Sippican) Inc.: WinMK21 Data Acquisition and Post Processing Software User's
1640 Manual P/N 352210, Rev. B, 134 pp, 2010.
- 1641 Lockheed Martin Sippican (Sippican) Inc.: MK21 Ethernet Surface 1U DAQ - Bathythermograph data
1642 acquisition system, installation and operation manual, P/N 352186, Rev. D, 47 pp, 2014.
- 1643 Sy, A.: XBT Measurements. In: WOCE Operations Manual, Part 3.1.3 WHP Operations and Methods, WHP
1644 Office Report, WHPO 91-1, 19 pp., 1991.
- 1645 Sy, A., and D. Wright: XBT/XCTD standard test procedures for reliability and performance test of expendable
1646 probes at sea. Revised draft. Geneva, Switzerland, WMO, TC SOT JCOMM Ship Observations Team, 8pp.
1647 DOI: <https://doi.org/10.25607/OBP-1487>
- 1648 Tan, Z., Reseghetti, F., Abraham, J., Cowley, R., Chen, K., Zhu, J., Zhang, B., and Cheng, L.: Examining the
1649 Influence of Recording System on the Pure Temperature Error in XBT Data. *J. Atmos. Oceanic Technol.*
1650 doi:10.1175/JTECH-D-20-0136.1, 2021.
- 1651 [Tan, Z., Cheng, L., Gouretski, V., Zhang, B., Wang, Y., Li, F., ... & Zhu, J. \(2023\). A new automatic quality
1652 control system for ocean profile observations and impact on ocean warming estimate. *Deep Sea Research Part
1653 I: Oceanographic Research Papers*, 194, 103961. <https://doi.org/10.1016/j.dsr.2022.103961>](#)
- 1654 Tanhua T, Pouliquen S, Hausman J, O'Brien K, Bricher P, de Bruin T, Buck JH, Burger EF, Carval T, Casey
1655 KS, Diggs S, Giorgetti A, Glaves H, Harscoat V, Kinkade D, Muelbert JH, Novellino A, Pfeil B, Pulsifer PL,
1656 Van de Putte A, Robinson E, Schaap D, Smirnov A, Smith N, Snowden D, Spears T, Stall S, Tacoma M,
1657 Thijsse P, Tronstad S, Vandenbergh T, Wengren M, Wyborn L and Zhao Z (2019) Ocean FAIR Data Services.
1658 *Front. Mar. Sci.* 6:440. doi: 10.3389/fmars.2019.00440
- 1659 Vignudelli, S., Cipollini, P., Reseghetti, F., Fusco, G., Gasparini, G.P., Manzella, G.M.R.: Comparison
1660 between XBT data and TOPEX/Poseidon satellite altimetry in the Ligurian-Tyrrhenian area, *Annales
1661 Geophysicae*, 21, 123-135, doi:10.5194/angeo-21-123-2003, 2003.
- 1662 K von Schuckmann, P-Y Le Traon, E Alvarez-Fanjul, L Axell, M Balmaseda, L-A Breivik, R J. W. Brewin,
1663 C Bricaud, M Drevillon, Y Drillet, C Dubois, O Embury, H Etienne, M Garcia Sotillo, G Garric, F Gasparin,
1664 E Gutknecht, S Guinehut, F Hernandez, M Juzo, B Karlson, G Korres, J-F Legeais, B Levier, V S. Lien, R
1665 Morrow, G Notarstefano, L Parent, A Pascual, B Pérez-Gómez, C Perruche, N Pinardi, A Pisano, P-M Poulain,
1666 I.M. Pujol, R.P. Raj, U Raudsepp, H Roquet, A Samuelsen, S Sathyendranath, J She, S Simoncelli, C Solidoro,
1667 J Tinker, J Tintoré, L Viktorsson, M Ablain, E Almroth-Rosell, A Bonaduce, E Clementi, G Cossarini, Q
1668 Dagneaux, C Desportes, S Dye, C Fratiani, S Good, E Greiner, J Gourrion, M Hamon, J Holt, P Hyder, J
1669 Kennedy, F Manzano- Muñoz, A Melet, B Meyssignac, S Mulet, B Buongiorno Nardelli, E O'Dea, E Olason,
1670 A Paulmier, I Pérez-González, R Reid, M-F Racault, D E. Raitos, A Ramos, P Sykes, T Szekely & N

- 1671 Verbrugge (2016) The Copernicus Marine Environment Monitoring Service Ocean State Report, Journal of
1672 Operational Oceanography, 9:sup2, s235-s320, <http://dx.doi.org/10.1080/1755876X.2016.1273446>
- 1673 [Wannamaker, B., 1980: XBT measurements near the sea surface: Considerations for satellite IR comparisons](#)
1674 [and data bases. Saclant ASW Research Centre Memo. SM-132, 13 pp.](#)
- 1675 Wilkinson, M., Dumontier, M., Aalbersberg, I. et al. The FAIR Guiding Principles for scientific data
1676 management and stewardship. Sci Data 3, 160018 (2016). <https://doi.org/10.1038/sdata.2016.18>
- 1677 Zodiatis, G., Drakopoulos, P., Brenner, S., & Groom, S. 2005. Variability of the Cyprus warm core Eddy
1678 during the CYCLOPS project. Deep Sea Research Part II: Topical Studies in Oceanography, 52(22-23), 2897–
1679 2910. <https://doi.org/10.1016/j.dsr2.2005.08.020>

Page 28: [1] Deleted	Microsoft Office User	6/6/24 3:55:00 PM
----------------------	-----------------------	-------------------

Page 30: [2] Deleted	Microsoft Office User	6/14/24 3:33:00 PM
----------------------	-----------------------	--------------------

▼
▲